



# Hiding among the palms: the remarkable discovery of a new palm bug genus and species (Insecta: Heteroptera: Thaumastocoridae: Xylastodorinae) from remote Norfolk Island; systematics, natural history, palm specialism and biogeography

Gerasimos Cassis<sup>A,\*</sup> , Geoff B. Monteith<sup>B</sup> and Anthony Postle<sup>C</sup>

For full list of author affiliations and declarations see end of paper

**\*Correspondence to:**

Gerasimos Cassis  
Evolution & Ecology Research Centre,  
School of Biological, Earth and  
Environmental Sciences University of New  
South Wales, Sydney, NSW 2052, Australia  
Email: [gcassis@unsw.edu.au](mailto:gcassis@unsw.edu.au)

**Handling Editor:**

Gonzalo Giribet

**Received:** 27 July 2023

**Accepted:** 20 September 2023

**Published:** 25 October 2023

**Cite this:**

Cassis G et al. (2023)  
*Invertebrate Systematics*  
37(10), 702–740. doi:[10.1071/IS23040](https://doi.org/10.1071/IS23040)

© 2023 The Author(s) (or their employer(s)). Published by CSIRO Publishing.

This is an open access article distributed under the Creative Commons Attribution-NonCommercial-NoDerivatives 4.0 International License ([CC BY-NC-ND](https://creativecommons.org/licenses/by-nc-nd/4.0/))

OPEN ACCESS

## ABSTRACT

The discovery of a remarkable new palm bug species on Norfolk Island brings into question its systematic position within the family Thaumastocoridae, and the validity and biogeography of the three extant subfamilies. *Latebracoris norfolcensis* gen. nov., sp. nov. is described from remote Norfolk Island in the Southwest Pacific. The species was found on the native Norfolk Island palm *Rhopalostylis baueri*. The formal description of the species includes fine details of external non-genitalic and genitalic characters, supported with images from light and scanning electron microscopy. Details of the egg are described, including the shape and micropylar configuration. All nymphal stages are diagnosed morphologically and morphometrically, with the segregation of the five instars using the Brooks–Dyar Rule. The natural history of the Norfolk Island Palm Bug is documented, including the oviposition site of eggs, and microhabitat of nymphs and adults on palm infructescences, with hypotheses about development in relation to reproductive succession of the palm host. The systematic position of the Norfolk Island Palm Bug is assessed through a phylogenetic analysis of a selection of taxa of the superfamily Miroidea, using the parsimony criterion. The phylogenetic analyses were partitioned into Recent and fossil taxa, revealing monophyly of the Thaumastocoridae, and the subfamilies Thaumastocorinae and Xylastodorinae, with synapomorphy and significant resampling support. The Thaicorinae are verified as synonymous with the Xylastodorinae. The monotypic fossil subfamily Thaumastotinginae is removed from the Thaumastocoridae and treated as *incertae familiae*. Suprageneric relationships were corroborated in the two taxon partition analyses. An overview of host associations is given verifying palm specialism for the Xylastodorinae. The natural history, palm specialism, biogeography, morphology and systematics of the Xylastodorinae and allies are discussed in light of the discovery of *Latebracoris norfolcensis*.

**ZooBank:** [urn:lsid:zoobank.org:pub:40A20DE4-6489-4B67-BF2E-0B7256BA1CD1](https://zoobank.org/urn:lsid:zoobank.org:pub:40A20DE4-6489-4B67-BF2E-0B7256BA1CD1)

**Keywords:** biogeography, biology, Heteroptera, host relationships, new species, systematics, Thaumastocoridae, Xylastodorinae.

## Introduction

Van Doesburg *et al.* (2010) reported the discovery of a new palm bug (Insecta: Heteroptera: Thaumastocoridae: Xylastodorinae) from New Caledonia, *Proxylastodoris kuscheli* van Doesburg, Cassis & Monteith, 2010, collected on *Burretiokentia vieillardii* (Brongn. & Gris) Pic.Serm (Arecaceae). This was the first extant palm bug species of Xylastodorinae recorded from the Eastern Hemisphere. We report in this work the discovery of a second Southwest Pacific xylastodorine species, *Latebracoris norfolcensis* gen. nov., sp. nov., from Norfolk Island. This suggests xylastodorine relictualism in the Southwest Pacific (van Doesburg *et al.* 2010). The fact that *Proxylastodoris kuscheli* is congeneric with the

Baltic amber species *Proxylastodoris gerdae* Bechly & Wittmann, 2000 (Bechly and Wittmann 2000) also indicates a broader Eastern Hemisphere biogeographic history (van Doesburg *et al.* 2010), with an Eocene minimum age (van Doesburg *et al.* 2010). This also suggests an ancestral and near cosmopolitan distribution for the Xylastodorinae, taking into account the Western Hemisphere Miocene species *Discocoris dominicanus* Slater & Baranowski, 2000 (Slater and Baranowski 2000) from Dominican amber and the recent transfer of the Indo-Malayan species *Thaicoris sedlaceki* Kormilev, 1969 to the Xylastodorinae (Schuh and Weirauch 2020).

Like the New Caledonian palm bug and the Western Hemisphere Xylastodorinae, *Latebracoris norfolcensis* is associated with palms (*viz.* *Rhopalostylis baueri* (Hook.f.) H.Wendl & Drude). This verifies palm specialism at a trans-oceanic scale (van Doesburg *et al.* 2010). Poinar and Poinar (1999) speculated palm affiliation for xylastodorines in the Eocene, in an era when palms were diverse in the Australian biogeographic region (Dowe 2010). Alternatively, xylastodorines are conceivably undersampled in the Eastern Hemisphere, with the recent New Caledonian (van Doesburg *et al.* 2010) and Norfolk Island discoveries. This suggestion is predicated on the inaccessibility of inflorescences and infructescences of many palm species at ground level, including those inhabited by xylastodorines (Couturier *et al.* 2002; van Doesburg *et al.* 2010). Anecdotally, heteropterists pay little attention to palms as hosts, with few palmivory records in the literature (Howard *et al.* 2001) and there is also a lack of evidence of palm specialism at the suprageneric level in the Heteroptera, aside from the Xylastodorinae (Couturier *et al.* 1998, 2002; Cassis *et al.* 1999).

*Latebracoris norfolcensis*, together with described fossil and extant species of Xylastodorinae, exhibit morphological stasis, spanning ~33 million years, with conserved somatic (e.g. flattened body, corial cells) and genitalic (e.g. pygophore asymmetry) characters. This likeness allows testing of the suprageneric classification of the Thaumastocoridae with integration of the classification of fossil and Recent taxa (*sensu* Szwedo 2016), albeit with limitations of fossil preservation (Cassis and Schuh 2010). Foremost is the status of the Thaicatorinae that Heiss and Popov (2002) transferred from the Piesmatidae to the Thaumastocoridae based on the asymmetrical male genitalia, maintaining its subfamilial ranking. On the contrary, Schuh and Weirauch (2020) considered the Thaicatorinae synonymous with the Xylastodorinae, given shared possession of pretarsal (i.e. presence of 'pulvilli') and genital (i.e. absence of parameres) characters. The classification of the Thaumastocoridae is also complicated by the work of Heiss and Golub (2015), who described a Burmese amber fossil, *Thaumastotingis areolatus* Heiss & Golub, 2015, assigning it to the Thaumastocoridae, in its own subfamily, the Thaumastotinginae. The discovery of *Latebracoris norfolcensis* provides an opportunity to ascertain its systematic position and impact on the classification of the infraorder

Cimicomorpha and superfamily Miroidea (*sensu* Schuh and Štys 1991).

The aims of this work are to: (1) formally describe *Latebracoris norfolcensis* gen. nov., sp. nov.; (2) document the natural history of this species, including all life stages on the palm host; (3) phylogenetically analyse the systematic position of *L. norfolcensis* in the cimicomorphan superfamily Miroidea, using exemplar taxa of suprageneric groups; (4) test the validity of the four Thaumastocoridae subfamilies (Thaumastocorinae, Xylastodorinae, Thaicatorinae and Thaumastotinginae); (5) assess palm specialism of the Xylastodorinae in relation to a tribal phylogeny of the palm family Arecaceae (Baker and Dransfield 2016); and (6) discuss the biogeography and conservation of *L. norfolcensis* on Norfolk Island.

### Palm associations and natural history of the Xylastodorinae

All Xylastodorinae feed on palms (Arecaceae), with 8 genera and 11 species of palms recorded as hosts (Barber 1920; Kormilev 1955; Baranowski 1958; Viana and Carpintero 1981; Slater and Schuh 1990; Couturier *et al.* 1998, 2002; Cassis *et al.* 1999; van Doesburg *et al.* 2010). The monotypic South-East Asian *Thaicoris* is the only genus of the four extant xylastodorine genera for which neither foodplant nor biology is known, with *T. sedlaceki* known from Thailand and Java (Heiss and Popov 2002). The biology of *Xylastodoris luteolus* Barber, 1920, in comparison to the other three xylastodorine genera is well known, which is a pest of the ornamental royal palm, *Roystonea regia* (Kunth) O.F.Cook that is native to Cuba and introduced to Florida (Baranowski 1958; Weissling *et al.* 2012). The elongated, flattened adults and nymphs live in narrow spaces between compressed and unexpanded leaflets, feeding on leaf tissues and laying eggs among surface vestiture of the leaflet midribs.

The remaining two genera, the New Caledonian *Proxylastodoris* van Doesburg, Cassis & Monteith, 2010 and the Neotropical *Discocoris* Kormilev, 1955, the latter with five described species, both occur on flowering or fruiting structures of palms. Adults and nymphs of *Proxylastodoris kuscheli* occur on both inflorescences and infructescences of *Burretiokentia vieillardii*, although further details of the biology are cursory (van Doesburg *et al.* 2010). *Discocoris* species are oval and greatly flattened, with explanate margins of the thorax and hemelytra such that the appendages are concealed beneath the body. Most records are from inflorescences or infructescences of palms (Couturier *et al.* 1998; Cassis *et al.* 1999). Couturier *et al.* (2002) investigated the biology of *Discocoris drakei* Slater & Ashlock, 1959 in detail, recording it from the palm *Oenocarpus mapora* Karsten in Belém, Brazil. Winged adults were found to arrive on young inflorescences when the male flowers first open in large numbers, feeding on the unopened female flowers and laying eggs in the fissure around the base of female flowers. The hatching nymphs feed

on the young female flowers, pass through five instars in 15–20 days, and by the time the fruit are forming have moulted to adults and leave the inflorescence. They recorded no palm bug activity on infructescences as fruit mature.

### Morphology of life stages of Xylastodorinae

Eggs have been described and illustrated for species exemplars of all extant xylastodorine genera except *Thaicoris*. In *Proxylastodoris kuscheli*, the illustrated ovarian egg, missing the operculum, is barrel-shaped and oval in cross-section and has an erect fringe of ~40 contiguous, subrectangular micropylar processes around the aperture (van Doesburg *et al.* 2010). The surface has a continuous raised, hexagonal pattern (van Doesburg *et al.* 2010). The egg of *Xylastodoris luteolus* is elongated, cylindrical, capped with a textured operculum without a fringe of micropylar processes and with the chorion having a fine hexagonal surface (Baranowski 1958; Cobben 1968; Weissling *et al.* 2012). In *Discocoris* species, the egg is erect and has a slightly curved urn-shape with the basal half slightly flattened and this is inserted into the fissure around the flower base. The chorion surface has hexagonal sculpturing, each hexagon having a minute pore in the centre. The operculum is circular and the opening lacks micropylar processes (Couturier *et al.* 2002). Cobben (1968) assessed the egg structure in *Xylastodoris luteolus* and *Discocoris* species.

Nymphal Xylastodorinae have been illustrated for all extant genera except *Thaicoris*. Instar V of *Proxylastodoris kuscheli* has wing buds reaching the rear margin of abdominal tergum 3 and a single dorsal scent gland opening slightly posterior to the border between abdominal terga 3 and 4 (van Doesburg *et al.* 2010). Slater and Schuh (1990) illustrated instar V of *Discocoris imperialis* Slater & Schuh, 1990 that has two scent glands, each with a single opening, at the anterior margins of abdominal terga 4 and 5. Couturier *et al.* (2002) state that for *D. drakei*, the two single-opening glands are at the anterior margin of abdominal terga 4 and 5 but the illustration seems to show these on terga 5 and 6. All instars are described and the first instars are noted to have a marginal fringe of specialised, stout, branched setae not recorded elsewhere in the family. *Xylastodoris luteolus* nymphs have two scent glands situated at the anterior borders of abdominal terga 4 and 5, each with ‘openings double but very close together’ (Schaefer 1969). The latter is the only xylastodorine with paired openings, though Schuh and Weirauch (2020) incorrectly state that this is a subfamily characteristic. All Thaumastocorinae where nymphs have been described have two abdominal scent glands, with single openings, situated at boundaries between abdominal terga 3/4 and 4/5 (e.g. Slater 1973). Cassis *et al.* (1999) placed these between abdominal terga 4/5 and 5/6 in *Onymocoris stysi* Cassis, Schuh & Brailovsky, 1999.

Adult xylastodorine species are diagnosed by the presence of antenniferous tubercles, an expanded costal area,

the corium reaching near the apex of the hemelytra, the presence of a metathoracic gland external efferent system, the absence of a tibial appendix, presence of pseudopulvilli and the absence of parameres (Drake and Slater 1957; Schuh and Štys 1991; Schuh and Slater 1995; van Doesburg *et al.* 2010). These characters readily differentiate these species from the Thaumastocorinae, with species of the latter lacking antenniferous tubercles, the eyes are usually strongly pedunculate and the left paramere is present (Drake and Slater 1957; Noack *et al.* 2011). Head characters exhibit variation within both thaumastocorid subfamilies, including the size and degree of dorsalisation of the mandibular plates (e.g. cf. Slater and Schuh 1990 for Xylastodorinae with Drake and Slater 1957 for Thaumastocorinae). The pronotum is not diagnostic for the subfamilies, with variation between genera in the Xylastodorinae. For example, the anterolateral margins in *Latebracoris norfolcensis* and *Discocoris* species project strongly in front of the eyes and as a result the head is deeply embedded in the pronotum (e.g. Slater and Schuh 1990), whereas the pronotum has a small anterolateral tubercle in *Proxylastodoris* species and the head is not embedded (van Doesburg *et al.* 2010). The hemelytron has pronounced differences in the Xylastodorinae, including in *Latebracoris norfolcensis*, with the median flexion line divergent from R + M, shortened in length and removed from the costal margin. In the Thaumastocorinae the median flexion line is adjacent to the costal margin and not distally divergent as in *Onymocoris stysi* (Cassis *et al.* 1999). By contrast, the hind wing shows little promise in determining relationships, with morphological homogeneity (Drake and Slater 1957; van Doesburg *et al.* 2010). The thaumastocorid hind wing also shares similarities with the Tingidae, although Lis (1999) illustrated ‘secondary veins’ between the two folds of the hind wing in Tingidae that are lacking in thaumastocorids reported on to date.

Documentation of the male and female genitalia is limited in the Xylastodorinae. Descriptions and illustrations for both are limited to *Xylastodoris luteolus* (Drake and Slater 1957) and *Proxylastodoris kuscheli* (van Doesburg *et al.* 2010). The aedeagus in both is composed of a mostly membranous endosoma that has elongated spicules in the former species and not in the latter. The female genitalia are poorly understood and characterised by simplicity, lacking an ovipositor (Drake and Slater 1957), uncertainty about the presence of a sperm storage organ and a membranous bursa copulatrix without sclerotisation (van Doesburg *et al.* 2010).

### Phylogenetics and classification of Thaumastocoridae and Miroidea

Historical treatments of the Thaumastocoridae have been provided by Schuh and Slater (1995), Cassis *et al.* (1999), Cassis and Gross (1995) and van Doesburg *et al.* (2010). The monophyly and systematic position of the Thaumastocoridae were first treated phylogenetically by Schuh and Štys (1991), who confirmed the placement of the Thaumastocoridae in the

infraorder Cimicomorpha, within the suprageneric group Miriformes. This comprised the Microphysidae, Joppeicidae, Miridae, Tingidae and Thaumastocoridae, with the latter three families placed in the herbivorous and subordinate superfamily Miroidea. Kerzhner (1981) erected an alternative sister-group relationship between the Tingidae and Thaumastocoridae but related these distantly to the Miridae; however, this was not based on an analysis of codified characters.

The monophyly and suprageneric position has also recently been tested with total evidence phylogenetic analyses of morphological and multilocus sequence partitions (Schuh *et al.* 2009; Weirauch *et al.* 2019), and a molecular only study (Tian *et al.* 2008). Schuh *et al.* (2009) confirmed the placement of the Thaumastocoridae within the Cimicomorpha and falsified the Miriformes, with the predaceous Microphysidae and Joppeicidae included in the superfamily Cimicoidea. These authors did not recover the Thaumastocoridae as a monophyletic group, with the Thaumastocorinae and Xylastodorinae distantly related to each other, and also far removed phylogenetically from the Tingidae + Miridae. By contrast, Weirauch *et al.* (2019) recovered the Miroidea as erected by Schuh and Štys (1991), in a RAxML analysis, with 90% resampling support, with the Thaumastocorinae and Xylastodorinae as sister-groups but with moderate support (72%). Morphological synapomorphies to support Miroidea were also found, including the elongated bucculae, fused lateral abdominal tergites and asymmetrical parameres that are all nonetheless contradicted within the superfamily. Tian *et al.* (2008) did not recover the Miroidea, with equivocal relationships for the Thaumastocoridae in both Maximum Likelihood and Bayesian analyses, albeit with a limited sample of nrDNA and rDNA sequences.

The classification and validity of the subfamily Thaicatorinae have received little attention. Heiss and Popov (2002) transferred *Thaicoris sedlaceki* from the pentatomorphan family Piesmatidae to the Thaumastocoridae, primarily on the basis of the unique male and female genitalia, and maintained its subfamilial status. Van Doesburg *et al.* (2010) commented on the shared pseudopulvilli between Thaicatorinae and Xylastodorinae, suggesting a sister-group relationship but requiring a cladistic analysis. Schuh and Weirauch (2020) considered the presence of pretarsal 'pulvilli' in *T. sedlaceki* as shared with the Xylastodorinae, synonymising the Thaicatorinae and effectively recognising the Xylastodorinae from tropical Asia for the first time.

### Fossil Xylastodorinae and Thaumastotinginae

Five fossil species are assigned to the Thaumastocoridae, two of which are from Dominican amber (Miocene) (*Discocoris dominicanus* and *Paleodoris lattini* Poinar & Santiago-Blay, 1997), two from Baltic amber (Eocene) (*Proxylastodoris gerdae* and *Thaumastotingis areolatus*) and

*Protodoris minusculus* Nel, Waller & de Ploëg, 2004 from Paris Basin amber (Eocene). Cassis and Schuh (2010) removed *P. minusculus* from the Thaumastocoridae, with the specimen poorly preserved and lacking the diagnostic characters needed to assign it to the Thaumastocoridae. The other four species are well preserved and their inclusion in the Xylastodorinae is defensible. Although *D. dominicanus* and *P. lattini* do not possess diagnostic genitalic characters, these species possess secondary characters (i.e. enlarged mandibular plates, explanate costal area) that are sufficient for testing inclusion in the Xylastodorinae.

Heiss and Golub (2015) tentatively assigned the fossil taxon *Thaumastotingis areolatus* to the Thaumastocoridae, in its own subfamily, the Thaumastotinginae. Shared characters with both the Tingidae (e.g. areolate paranota and hemelytra, and wing venation) and Thaumastocoridae (e.g. absence of pronotal carinae, asymmetrical male genitalia, 'pulvilli' as in Xylastodorinae) were reported.

### Norfolk Island and conservation of *Latebracoris norfolcensis*

Norfolk Island is an oceanic island of ~35 km<sup>2</sup> that is ~3 million years old, originating on the Norfolk Island Ridge (Holloway 1977, 1990). The island has biogeographic significance, given its remoteness, ~1400 km east of northern New South Wales, ~750 km SSW of New Caledonia and ~750 km NNW of New Zealand (Holloway 1977). Norfolk Island was a subtropical island with closed canopy vegetation prior to European habitation (Rentz 1988) but has been subject to extensive land clearance, with only ~5% of native vegetation remaining (Macphail *et al.* 2001), coupled with the deleterious impacts of invasive species (Holloway 1977, 1982; Green and Wilson 1994). A great deal of the native biota is now restricted to the Norfolk Island National Park (Director of National Parks 2010, 2018). The confinement of *Latebracoris norfolcensis* sp. nov. within the 460 ha (13% of area of island) of the national park has conservation importance given its extreme narrow range and putative phylogenetic endemism.

## Materials and methods

### Materials

This study is based on examination of 297 specimens. The specimens are housed in the following institutions: AM, Australian Museum, Sydney; ANIC, Australian National Insect Collection, Canberra; AMNH, American Museum of Natural History, New York; MNHN, Muséum national d'Histoire naturelle, Paris; NHM, Natural History Museum, London; QM, Queensland Museum, Brisbane; UNSW, University of New South Wales, Sydney. Specimens for the phylogenetic analysis were borrowed from the AMNH, AM and QM.

## Palm host distribution, habitat and reproductive biology

The only known foodplant of *Latebracoris norfolcensis* is *Rhopalostylis baueri*, the sole native palm of Norfolk Island. The only other natural occurrence of this palm is in the oceanic Kermadec Islands, 1370 km east of Norfolk Island (Dowe 2010). The only congener is *Rhopalostylis sapida* (Sol ex G.Forst) H.Wendl & Drude, a native palm in New Zealand that occurs widely on both the North Island and the northern half of the South Island, and on Chatham Island, where it is the most southerly palm species known (Salmon 1986).

Dowe (2010) summarised the phylogenetic relationships of Australian palm genera. He related *Rhopalostylis* H.Wendl & Drude with the Lord Howe Island monotypic and endemic genus *Hedyscepe* H.Wendl & Drude in the subtribe Rhopalostyliinae, which is sister to the subtribe Archontophoenicinae that also has a number of genera in Australia and New Caledonia. *Burretiokentia* Pic.Serm., host

to the New Caledonian *Proxylastodoris kuscheli*, belongs to the related subtribe Basseliniinae, which comprises the Lord Howe monotypic and endemic genus *Lepidorrhachis* (H.Wendl & Drude) O.F.Cook and other genera on Southwest Pacific islands but not from the Australian mainland (Pintaud and Baker 2008). The Norfolk Island palm is a tall, slender, single-stemmed monoecious palm, reaching 18 m in height that grows abundantly within the preserved forest areas of the island and is especially common along the valley floors within the National Park (Fig. 1). Palms that grow in full light beside roads and tracks through the forest may be very short, and bear flowers and fruit close to the ground. (Fig. 2c, d)

Morphological palm terms are defined here to facilitate later discussion on palm bug biology. The leaves have pinnate leaflets arranged along the terminal shaft-like *petiole* that is attached to the trunk by a tubular *crownshaft*. When the palm reaches maturity, a complex branched *inflorescence* develops inside the crownshaft in a sac-like structure (the *spathe*) formed by two enclosing bracts at the base of the

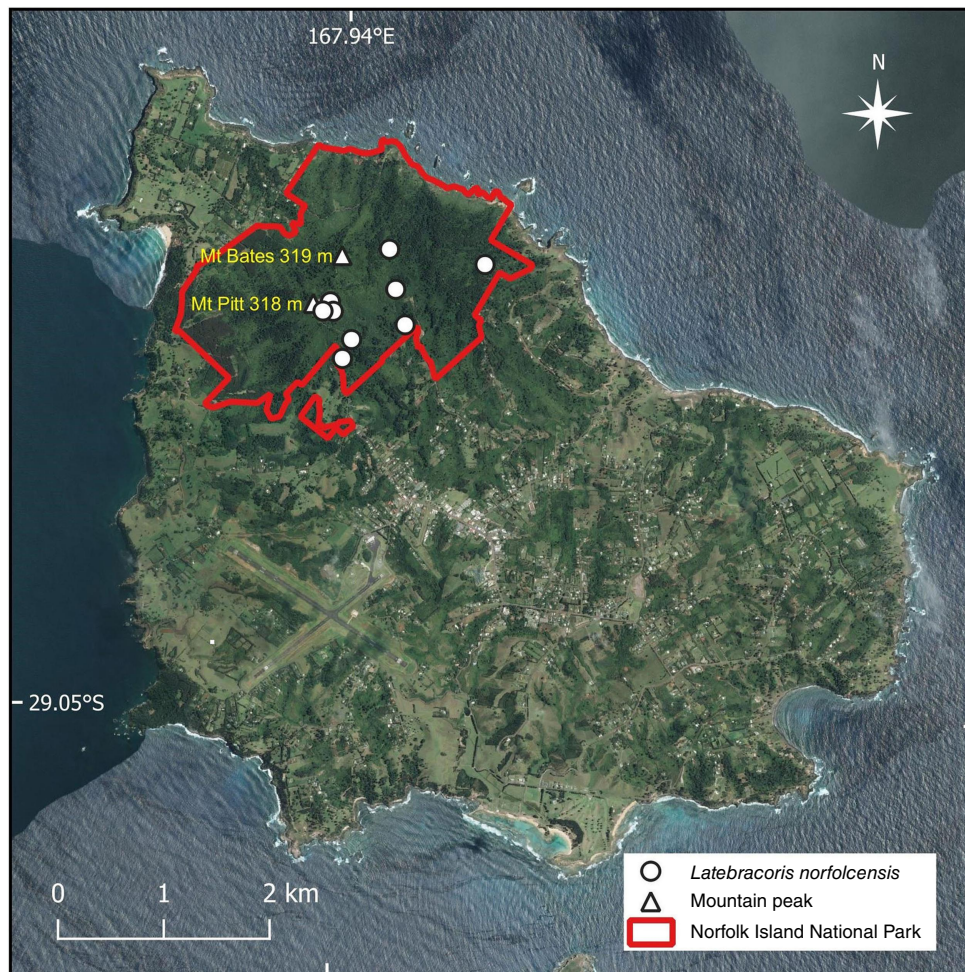


**Fig. 1.** Nine localities of *Latebracoris norfolcensis* sp. nov. within Norfolk Island National Park, where most of the intact forest occurs on the island. Norfolk Island forest remnants outside the National Park were not sampled for the Norfolk Island palm bug.



**Fig. 2.** Field collecting of *Latebracoris norfolcensis* sp. nov. on the palm, *Rhopalostylis baueri*, on Norfolk Island. (a) Detail of net used to spray with cord-activated pyrethrin aerosol to collect thaumastocorids from high infructescences of the palm. (b) Geoff Monteith using the net to collect on lower palms. The handle could be extended to 6 m for higher palms. (c) Tony Postle beside the very short palm on which the first specimens were collected in 2019. The blue sheets are for catching falling bugs after hand spraying infructescences with aerosol pyrethrin. (d) *Rhopalostylis baueri* bearing four sequential axillary infructescences. Green fruit are the youngest (IF), red fruit on the right are in the second stage of development, scattered fruit on the left are at the third stage of development and old withered rachillae, lacking fruit are in foreground. Abbreviations: EN, extension handle; IC, insect aerosol can; NE, net.

inflorescence (Fig. 3e). When the leaf is shed, the spathe is exposed and the two bracts are shed allowing the primordial inflorescence to expand into a complex structure of which the terminal branches are termed *rachillae*. These are initially white and bear the separate male and female flowers. After pollination the male flowers are shed and the female flowers

develop to hard spherical, berry-like *fruit* (that are technically *drupes*). The inflorescence is subsequently termed an *infructescence*. Bases of the individual fruit are inserted into a circular depression in the rachilla known as the *cupule* and surrounded by a basal cirlet of six overlapping brown *perianth scales* that are the hardened petals and sepals of the flowers (Fig. 2d, 3).



**Fig. 3.** Microhabitat and host of *Latebracoris norfolcensis* sp. nov. (a) Cryptic adult (yellow arrow) on infructescence rachilla of *Rhopalostylis baueri*, concolourous with perianth scales. Red arrows indicate fissure around base of fruit where eggs are laid. (b) Adult apparently feeding on green rachilla of *R. baueri* while positioned to resemble perianth scales. (c) Adult on infructescence rachilla. (d) Adult resting in cupule from which fruit has been shed. (e) Unopened *Rhopalostylis baueri* spathe, in foreground, under which adults were aggregated.

The fruits are initially white, subsequently turn green and finally bright red at maturity (Fig. 2d, 3a–c). The rachillae also turn green when fruit are set (Fig. 3a–c).

### Fieldwork

*Latebracoris norfolcensis* was collected in the Norfolk Island National Park, at nine locations (Fig. 1). The initial collection of seven specimens of the Norfolk Island palm bug was made by Anthony Postle by beating the infructescences of a low specimen of the palm *Rhopalostylis baueri* beside a rainforest walking track in December 2019 (Fig. 2c); these specimens were collected serendipitously while searching for anthocorid bugs. Upon return to Australia, Geoff Monteith (Queensland Museum) recognised this as a new

thaumastocorid palm bug, having been an author and collector of the New Caledonian palm bug, *Proxylastodoris kuscheli* (van Doesburg et al. 2010). Postle and Monteith revisited Norfolk Island in the period 2–9 February 2021 and resurveyed the palm host in the Norfolk Island National Park under Permit Number NINP 2020/R/03 to Anthony Postle. Success in collecting the New Caledonian species came from spraying low fruiting and flowering palms with hand-held cans of rapid-breakdown aerosol pyrethrin and collecting falling palm bugs on sheets spread on the ground (Fig. 2c; also see van Doesburg et al. 2010, fig. 43 for *Proxylastodoris kuscheli* knockdown method).

However, since most palms on Norfolk Island were expected to be much taller, an extensible insect net device was built in Brisbane. A 70-cm diameter butterfly net hoop

with a 1 m deep bag of fine voile fabric was attached to a telescopic handle that extended to 6 m (Fig. 2a, b). The hoop was bent back at 45° so the net could be more easily slipped over a large hanging palm infructescence when the net was raised vertically. A cylindrical aerosol can holder with a simple lever device that could depress the button on the aerosol by pulling a cord that led down through ferrules to the user (Fig. 2a) was attached on the handle at the base of the hoop.

At the time of the visit, no palms had new flowers but most had fruit of various ages (Fig. 2d). In the field individual infructescences were sprayed with the pyrethrin aerosol as the extended net was slipped over and subsequently held in position for several minutes while insects and debris fell into the net. Several infructescences were treated in this way before lowering the net for collection. Net contents were transferred to ethanol and searched under a stereomicroscope for palm bugs. Very low fruiting palms were sprayed directly and bugs collected from sheets spread on the ground (Fig. 2c). These aerosol methods proved highly successful. Low unsprayed infructescences were examined directly for insects in the field and one whole infructescence was collected and systematically searched under a stereomicroscope for insects and eggs. Low numbers were taken in this way.

During the February 2021 visit, extensive beating of other plants was undertaken, malaise traps were run, sifted leaf litter was processed through Berlese funnels, and pyrethrin spraying of logs and tree trunks was carried out. None of these methods yielded the xylastodorine palm bug. James Tweed commenced a PhD project at the University of Queensland on insect conservation on Norfolk Island at the beginning of 2022. We briefed him on the new xylastodorinae that he located at two localities by beating low palms in February and September 2022, and at a third locality he found a specimen in a malaise trap in September 2022. Tweed saw an adult on palm rachillae in February 2023 and nymphs in March 2023. All study sites are within the Norfolk Island National Park where Tweed's collecting is covered by Permit Number 'James Tweed 2/9/22–30/4/23'. Glynn Maynard, a retired entomologist living on Norfolk Island, made visual observations of nymphs of the palm bug resting in cupules in May and June 2023.

## Morphometrics

Standard taxonomic measurements were taken of 10 males, including the holotype and nine females, in millimetres with a 10× eyepiece graticule attached to a Leica M3Z stereomicroscope. The adult measurements are given in the *L. norfolcensis* species description.

Head widths across the outer margin of eyes and body length from the apex of the clypeus to the tip of the abdomen were taken of 130 nymphs from a single collection. These data were used for plotting size distribution of the nymphal instars using the procedures of the Brooks–Dyar Rule (Floater 1996).

## Genitalic preparation

The male genitalia were macerated in 5% KOH and washed in distilled water. The pygophore was removed from the abdomen and further dissected, and the aedeagus was heated in lactic acid and the endosoma was partly expanded. The male genitalia were illustrated using a Leica DMB compound microscope. The female genitalia were also macerated as above. The abdominal terga were removed, and the bursa copulatrix, oviducts and ovarioles in part were examined and illustrated. The terminology follows van Doesburg *et al.* (2010) in part. We recognised two distinct regions of the ductus seminis for the male aedeagus: the basal annulated component we refer to as the ductus seminis proximalis and the distal component with tile-like sclerotisation as the ductus seminis distalis.

## Imaging

Field photographs of habitats and live specimens were taken with a Canon SX1100 camera (Monteith) and an Olympus TG-5 (Tweed). Habitus photographs were taken at the Queensland Museum on a Visionary Digital BK-Plus imaging system, using a Canon 5DS camera. Focus stacking was done with Zerene Stacker software, and edited with Photoshop and Topaz AI software.

Scanning electron micrographs were produced at the University of NSW using a Hitachi TM3000 desktop scanner. Specimens were uncoated and imaged at low voltage. Morphological adult and egg characters were imaged using the scanning electron microscope (SEM) and TM3000 software (ver. 02-01, see <https://www.hitachi-hightech.com/file/us/pdf/library/literature/TM3000-TableTopSEM-BrochureHTD-E188Q.pdf>).

## Phylogenetics

The phylogenetic analysis in this work presupposes the superfamily Miroidea as a monophyletic group, following Schuh and Štys (1991), Weirauch *et al.* (2019) and phylogenomic results in progress (Cassis *et al.*, in prep.). The main hypotheses tested herein are: (1) Miridae + Tingidae are sister taxa (Schuh and Štys 1991; Schuh *et al.* 2009); (2) Tingidae + Thaumastocoridae are sister taxa (Kerzhner 1981); (3) Thaumastocoridae is a monophyletic group (Schuh and Štys 1991); (4) Thaumastocoridae is not a monophyletic group (Schuh *et al.* 2009); (5) Thaumastotinginae is a member of Thaumastocoridae (Heiss and Golub 2015); (6) Thaicatorinae is synonymous with Xylastodorinae (Schuh and Weirauch 2020); (7) Thaumastocorinae and Xylastodorinae are monophyletic groups (Schuh and Štys 1991; Schuh *et al.* 2009; Weirauch *et al.* 2019); and (8) the suprageneric relationships in the (a) Recent only, and (b) Recent and fossil taxon partitions in this work are corroborated. Genus-group monophyly and relationships in the Thaumastocoridae are not exhaustively tested, as only exemplar taxa were codified.

Taxon representatives of the three Miroidea families (Miridae, Thaumastocoridae and Tingidae) were analysed.

The Recent species by suprageneric taxa were: (1) Miridae (*Dicyphus famelicus* (Uhler, 1878), and *Trilaccus mimeticus* Chan & Cassis, 2019); (2) two species of Vianaidinae (*Anommatocoris araguanus* Guidoti, Montemayer, Campos & Guilbert, 2020, *Pterovianaida melchiori* Guidoti, Montemayer, Campos & Guilbert, 2020); (3) two species of Tingidae: Tinginae; Tingini (*Epimixia vulturina* Kirkaldy, 1908, *Inoma stysi* Cassis & Symonds, 2008); (4) four species of Tingidae: Cantacaderinae (*Allocader cordatus* (Hacker, 1928), *Cantacader* sp., *Carldrakeana socia* (Drake & Ruhoff, 1961), *Ceratocader* sp.); (5) two species of Tingidae: Tinginae: Phatnominae (*Phatnoma hackeri* Drake, 1928, *P. pacifica* Kirkaldy, 1908); (6) six species of Thaumastocoridae: Thaumastocorinae (*Thaumastocoris hackeri* Drake & Slater, 1957, *Thaumastocoris petilus* Drake & Slater, 1957, *Baclozygum bergrothi* Drake & Slater, 1957, *Baclozygum depressum* Bergroth, 1909, *Onymocoris barberi* Drake & Slater, 1957 and *O. stysi* Cassis, Schuh & Brailovsky, 1999); and (7) six species of Thaumastocoridae: Xylastodorinae (*Discocoris drakei*, *D. fernandesi* Slater & Brailovsky, 1983, *Latebracoris norfolcensis* sp. nov., *Proxylastodoris kuscheli*, *Thaicoris sedlaceki* and *Xylastodoris luteolus*). The following fossil taxa were codified from the literature: (1) *Thaumastotisingis areolatus* (Thaumastocoridae: Thaumastotisinginae); and (2) three species of Thaumastocorinae: Xylastodorinae (*Discocoris dominicanus*, *Paleodoris lattini* and *Proxylastodoris gerdae*). Trees were rooted with *Nabis kinbergii* Reuter, 1872 (Nabidae: Nabinae).

Phylogenetic analyses were conducted on exemplars of the 3 families of the Miroidea, based on codification of 65 unordered morphological characters for 31 species, in two taxon partitions: (1) Recent taxa only, and (2) Recent and fossil taxa. The data matrix was prepared in Mesquite software (ver. 3.5, see <http://www.mesquiteproject.org>) and is given in Table 1. The phylogenetic analyses were based on the parsimony criterion, conducted in TNT (ver. 1.5, see <https://www.lillo.org.ar/phylogeny/tnt/>; Goloboff and Catalano 2016), with New Technology default settings for Sectorial search and Tree fusing, and the Ratchet set at 1000 iterations. Analyses were conducted with equal (EW) and implied (IW) weights. For IW, the *K* value was set at 3, 5, 7, 10 and 100, with the most consistent tree topology used for resampling and character optimisation. The tree length for the minimal tree was calculated in TNT. For both taxon partitions, the IW minimal tree was subject to symmetrical resampling estimation with 10 000 replications. Character optimisation was produced in TNT. The tree file was transferred to Mesquite to calculate the consistency (CI) and retention (RI) indices. The data matrix and tree file were transferred to Winclada (ver. 1.00.08, see [www.diversityoflife.org/winclada](http://www.diversityoflife.org/winclada); Nixon 2002) to produce graphical depiction of the trees. The two trees in the Phylogenetic analyses section (see Fig. 13 and 14) give the character state transformations for each node, with uncontradicted synapomorphies in closed circles (each with character number above

and character state below each circle); contradicted synapomorphies are given in open circles, including on branches to terminal taxa. Resampling values >50% are given in black circles for nodes in Fig. 13 and 14 in the Phylogenetic analyses section, and are considered significant.

The morphological characters were codified for the abovementioned taxa, based on new observations and characters drawn from phylogenetic analyses of Schuh and Štys (1991; Cimicomorpha), Lis (1999; Tingidae s.l.), Guilbert (2001; Tingidae s.l.), Schuh et al. (2006; Miroidea), Schuh et al. (2009; Cimicomorpha), Guilbert et al. (2014; Tingidae s.l.), Weirauch et al. (2019; Cimicomorpha) and Guidoti et al. (2020; Vianaidinae). These were largely verified for the study taxa and supplemented with confirmation from seminal works, including Drake and Davis (1960), Kumar (1964), van Doesburg et al. (2010) and Golub and Popov (2016). Although there are egg and nymphal characters that may have phylogenetic value, evidence of these is fragmentary at the species level and are therefore excluded from the analysis. Substantial character state inapplicability exists for the fossil taxa in the dataset given their absence, particularly for genitalia of both sexes.

The character and character states are given in the results section, preceding the phylogenetic results.

## Results

### Biology

#### Natural history

A total of 27 males, 21 females, 249 nymphs and 11 batches of eggs of the Norfolk Island palm bug were collected during fieldwork in 2019–2020. All except one adult, which was taken in a malaise trap, were collected on infructescences of *Rhopalostylis baueri*. The first individual palm sampled in February 2021 was the same plant from which the initial chance collection was made in December 2019 (Fig. 2c). This bore four post-flowering low infructescences of different ages (Fig. 2d), three of which bore fruit of various ages and could be examined directly at head height. No adults or nymphs were detected after close visual examination for 15 min by G. B. Monteith and A. Postle. Sheets were subsequently spread on the ground and the infructescences sprayed with aerosol pyrethrin. This yielded 10 adults (e.g. Fig. 3a–c) and 83 nymphs of all instars, demonstrating the crypsis of this xylastodorine species and how difficult the bugs were to detect by eye (e.g. Fig. 3d).

Fruiting rachillae from the same palm were taken for microscopic examination on the same day, yielding several batches of eggs. These were all inserted around the base of the fruit in the narrow fissure between the outer surface of the petiolar scales and the raised edge of the cupule in the rachilla surface where the fruit develops (Fig. 3a–d). Eggs were most often deposited in tight-spaced single rows of up to seven eggs in a linear configuration (e.g. Fig. 4a–f), albeit

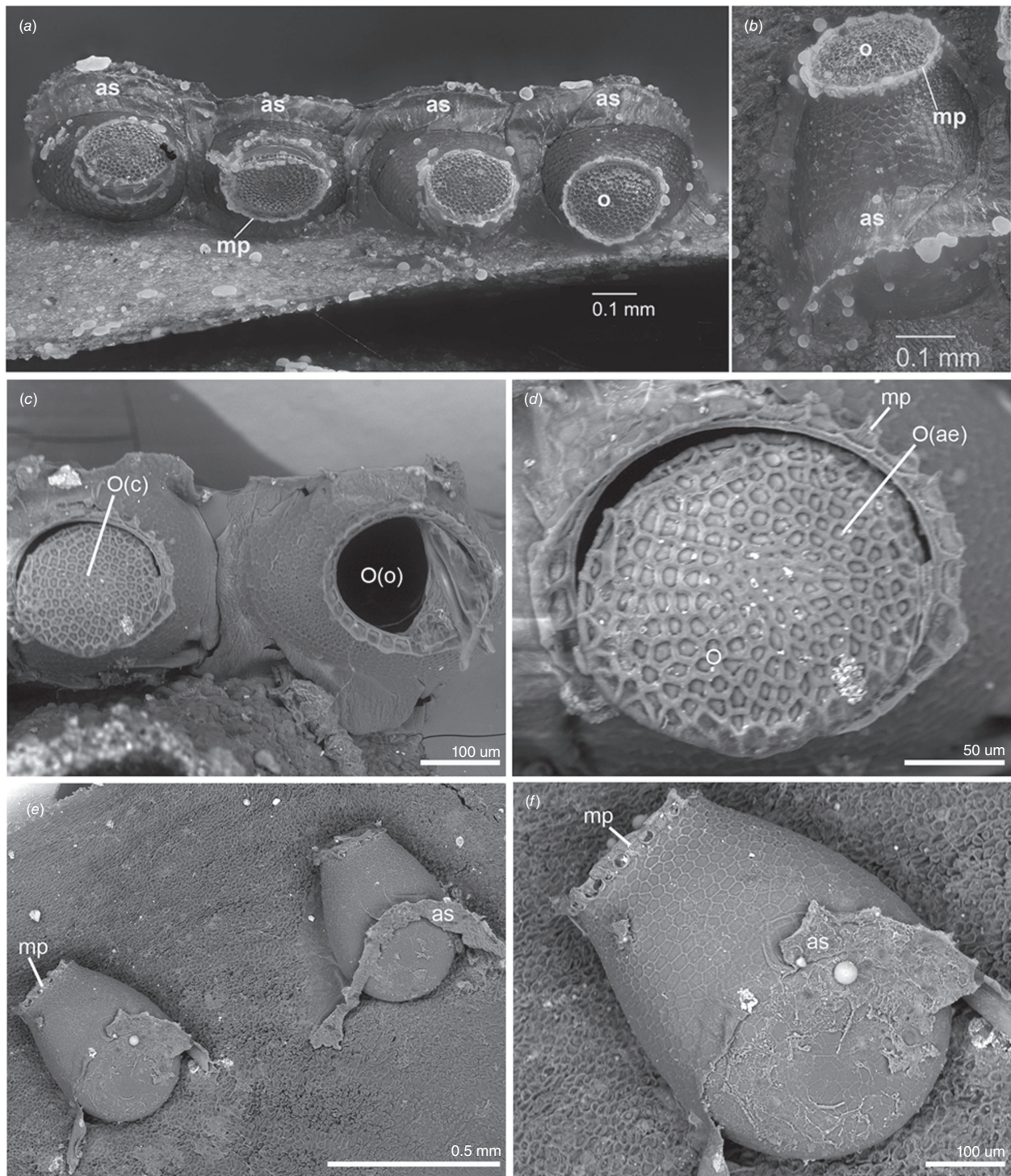


**Fig. 4.** Eggs and oviposition sites of *Latebracoris norfolcensis* sp. nov. (a) Dorsal view of a row of four eggs deposited on surface of a basal perianth lobe of *Rhopalostylis baueri* fruit and embedded in adhesive secretion. (b) Lateral view of an egg. (c) Scanning electron microscope (SEM) image of closed (left) and ecloded (right) eggs. (d) SEM image of aerolate fine structure of operculum. (e) Pair of eggs laid on *R. baueri*, with remnant of adhesive secretion. (f). Higher magnification of egg in lateral view, with fine structure of micropylar process. Abbreviations: as, adhesive secretion; mp, micropylar process; o, operculum; O(c), operculum closed; O(o), operculum open, egg apparently ecloded; O(ae), aerolate fine structure of operculum.

the occasional presence of single eggs. Eggs were always lodged in a droplet of adhesive secretion that coated the side of the egg against the petiolar scale and embedded approximately the lower third of the egg, with the operculum of the egg free (Fig. 4*b, e, f*). A clear boundary is visible between the adhesive associated with each egg, implying that the female deposits a separate droplet of adhesive for each egg.

Subsequent to these initial observations, rachillae from unsprayed palms were examined under the microscope and living adults were located, almost always resting on the petiolar scales (Fig. 3*a–c*). Adults were sometimes seen moving between the scales on the green surface of the rachillae but only once on the surface of a fruit.

A developing palm spathe is exposed when a leaf has recently been shed (Fig. 3*e*). This develops as a leaf axillary structure under a sheathing leaf base. When the leaf is finally shed from the tree, the spathe expands, splits open and the branched inflorescence is exposed, and subsequently flowers and sets fruit. We found a cluster of a dozen adult palm bugs under the new spathe when we pulled this away from the trunk. We postulate that the palm bugs that bred on the old inflorescence have migrated to beneath the new inflorescence, awaiting opening.

## Morphology

### Egg morphology

The eggs of *Latebracoris norfolcensis* are shiny, dark brown, urn-shaped, taper a little at top and bottom (Fig. 4*a–f*) and are slightly flattened at the widest part. The egg has a height of 0.5 mm, the widest diameter 0.34 mm and narrowest diameter 0.25 mm. The operculum (Fig. 4*a–d*) is flat, circular, 0.19 mm in diameter and bordered by ~30 close-set, subquadrangular processes, and has an areolate texture, with the raised margins of each areole hexagonal in outline (Fig. 4*a–f*).

### Nymphal morphometrics and morphology

All nymphal instars of *Latebracoris norfolcensis* are greatly flattened and semi-transparent with bright red eyes, with all preserved specimens having a yellow colour, with alternating transverse brown and reddish stripes on the abdomen (Fig. 5*b, c*). The antennae are yellowish-brown, with darker brownment on AII and apex of AIV in later instars.

Dorsal views of each instar are shown in Fig. 5. A single, red, dorsal abdominal scent gland is conspicuously present in all instars (Fig. 5*a*). This consists of a subspherical reservoir within abdominal segment 4 that opens to a single subcircular aperture slightly posterior to the anterior margin of abdominal tergum 5. In all instars the labium reaches to slightly beyond the hind margin of the metacoxae and is four-segmented in later instars.

Following the procedures of the Brooks–Dyar Rule (Floater 1996), both head width across the eyes and overall head–body length provided segregation into five discrete instars (Fig. 6). Size range (L, body length from apex of

clypeus to tip of abdomen in millimetres) and the following morphological attributes that also differentiate the five instars are as follows.

**First instar (Fig. 5*b*).** L, 0.90–1.17; antenniferous tubercle a minute, simple lobe with weakly angulate apex; lateral margin of pronotum, a narrow carina; sides of body fringed with long, fine, simple setae (as long as tibial diameter) each arising from a small tubercle and at a density of 2–3 per body segment.

**Second instar (Fig. 5*b*).** L, 1.30–1.50; antennifer a flattened lobe with two angled corners, but not forked; pronotum with prominent explanate margin, becoming larger in subsequent instars; fringing setae on sides of body shorter than tibial diameter and becoming relatively shorter in subsequent instars.

**Third instar (Fig. 5*c*).** L, 1.93–2.08; antennifer forked and becoming more so in subsequent instars; apex of maxillary plate slightly bent mesially at apex and becoming more so in subsequent instars.

**Fourth instar (Fig. 5*c*).** L, 2.62–2.87; short mesonotal wing buds present, not extending posteriorly beyond metanotum; explanate margin of pronotum and mesonotum weakly serrate; anterior angles of pronotum extending forward to level of centre of eye.

**Fifth instar (Fig. 5*c*).** L, 3.54–3.82; prominent wing buds present on both meso- and metanotum, reaching posteriorly to hind margin of abdominal segment III; antenniferous tubercle medially arcuate, and widely separated from the lateral margins of the clypeus; thoracic margins strongly serrate; anterior angles of pronotum extending forward to anterior margin of eye or beyond.

The adult morphology is given in the formal taxonomic description below.

## Taxonomy

Family **THAUMASTOCORIDAE** Kirkaldy, 1908

Subfamily **XYLASTODORINAE** Barber, 1920

***Latebracoris*** Cassis, Monteith & Postle, gen. nov.

(Fig. 1–15.)

ZooBank: [urn:lsid:zoobank.org:act:F20F61E8-D94C-4063-BCB7-229E0B8C2CB7](https://zoobank.org/urn:lsid:zoobank.org:act:F20F61E8-D94C-4063-BCB7-229E0B8C2CB7)

### Type species

*Latebracoris norfolcensis* Cassis, Monteith & Postle sp. nov., by original designation.

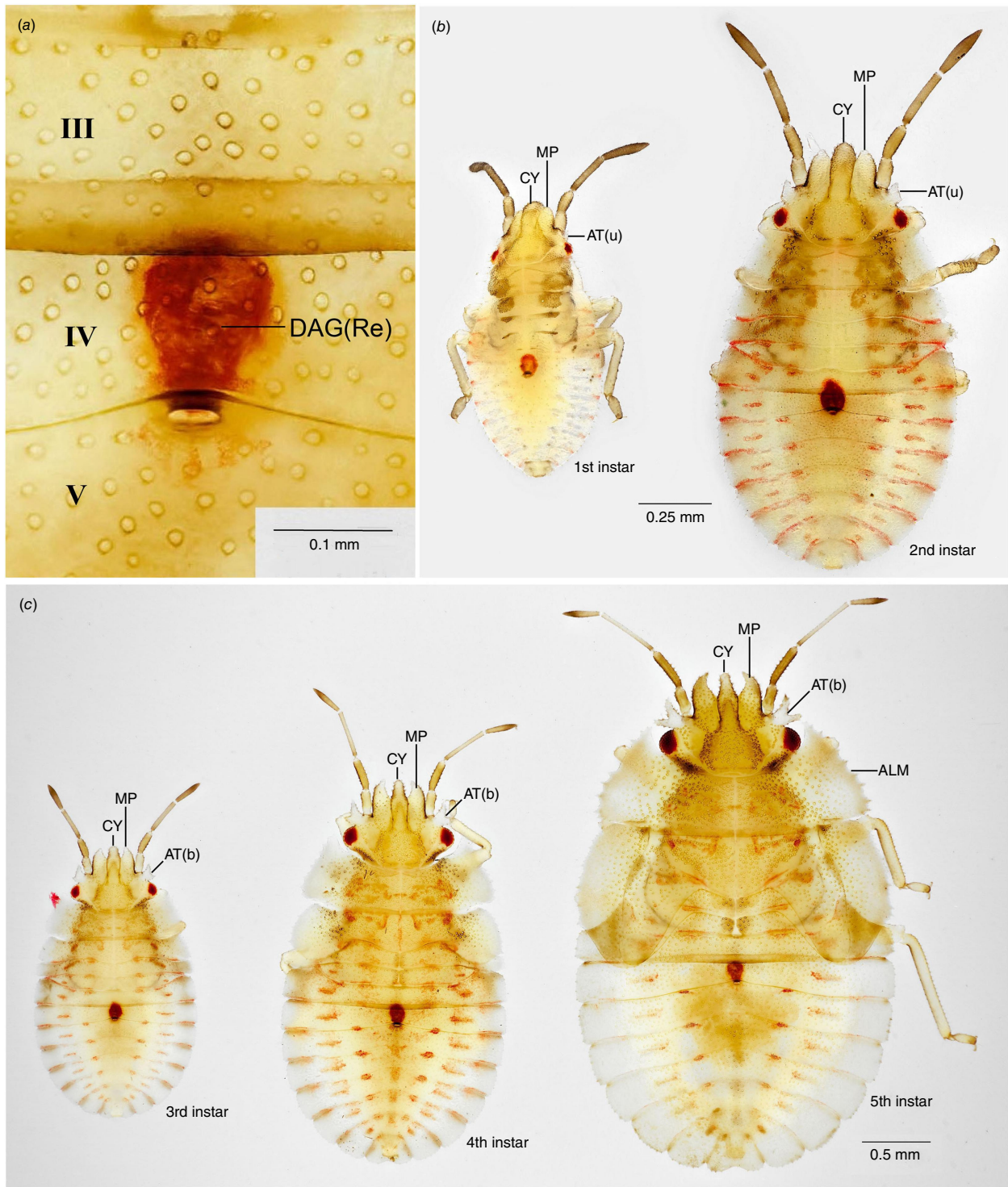


**Fig. 5.** Dorsal view of nymphal stages and dorsal abdominal gland of *Latebracoris norfolcensis* sp. nov. (a) Detail of dorsal abdominal scent gland of fifth instar; (b) First and second instar; (c) Third to fifth instars. Abbreviations: AT(b), antenniferous tubercle, apically bifurcate; AT(u), antenniferous tubercle, apically undivided; ALM, anterolateral margin of pronotum; CY, clypeus; DAG(Re), dorsal abdominal gland reservoir; MP, mandibular plate; III-V, abdominal terga III-V.

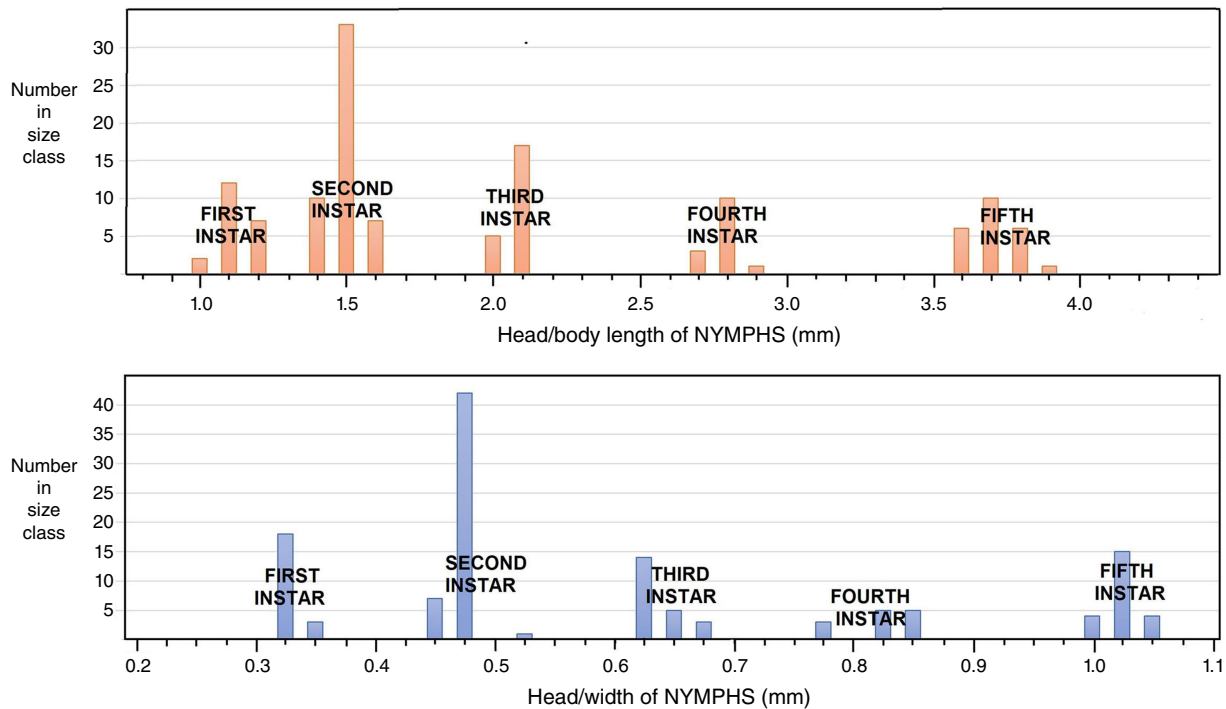


**Fig. 6.** Size class distribution of *Latebracoris norfolcensis* sp. nov. segregated into five instars, based on head/body length (top) and head width (bottom) measurements of 131 nymphs taken in a single pyrethrin collection.

## Etymology

Prefix from the Latin ‘*latebra*’ meaning hidden, in reference to the cryptic habit and the suffix ‘*coris*’ meaning bug; noun in apposition.

## Diagnosis

*Latebracoris* is recognised by the following combination of characters: body ovoid (Fig. 7a, b), strongly dorsoventrally flattened; ocelli postocular (7A); eyes small, suboval, substylate (Fig. 7a, b, 8a); labium reaching abdominal SIII; acute anterolateral angles of pronotum projecting well beyond posterior margin of head, reaching near anterior margin of eyes; bifurcate antenniferous tubercles present (Fig. 7a, b, 8a); abdominal sterna III and IV long (Fig. 7b); without tibial appendix (Fig. 9e); tarsi with apical spinose comb (Fig. 9e); pretarsus with elongated lamellate pseudopulvilli (Fig. 9f); hemelytra with short median flexion line (Fig. 10a); costal area broad, with corium reaching tip of hemelytron (Fig. 10a); corium with four cells (Fig. 10a); male abdominal SVIII and pygophore asymmetrical, latter right oriented (Fig. 7b, d, 11a); external female genitalia absent (Fig. 12b).

## Description

Body strongly dorsoventrally flattened, ovoid in shape (Fig. 7a, b). *Head*: preocular region strongly dissected,

apically with tripartite outline (Fig. 7a, b, 8a, b); mandibular plates arcuate, widely separated, subequal in length to clypeus (Fig. 7a, b, 8a); clypeus conical, tapered apically, extending posteriorly to near anterior margins of eyes, lateral margins weakly sinuate, margins posteriorly contiguous with weak grooves, leading to ocelli (Fig. 7a, b, 8a); bifurcate antenniferous processes, extending to near apices of first antennal segment, anterior branch longest (Fig. 7a, b, 8a); postocular region of head with margins strongly convergent posteriorly, sublinear (Fig. 7a, b, 8a); maxillary plates subtriangular, ventral in position, posterior margin obsolete; genae depressed; bucculae elongated, subparallel, almost reaching posterior margin of head, carinate (Fig. 8b). *Eyes and ocelli*: eyes suboval, substylate; ocelli postocular, widely separated (Fig. 7a, b, 8a). *Antennae*: 4-segmented; antennal length formula: AIII > AII > AIV = AI; AI extending anteriorly of antenniferous tubercle, subcylindrical, thickest segment; AII subcylindrical, little thinner than AI, weakly bowed; AIII and AIV subequal in thickness, thinner than AII; AIII cylindrical; AIV elongated, weakly fusiform (Fig. 7a, b). *Labium*: 4-segmented; LI shorter than bucculae, broadest segment, not dilated; LII–LIV subequal in length; LII bicompressed, reaching near posterior margin of prosternum; LIII–LIV flattened; LIII reaching near posterior margin of metasternum; LIV reaching near posterior margin of abdominal sternum III (Fig. 7b, 8b). *Pronotum*: exaggerated, with lateral margins explanate, anterolaterally projected near front of eyes, apically acute, posterolaterally short;

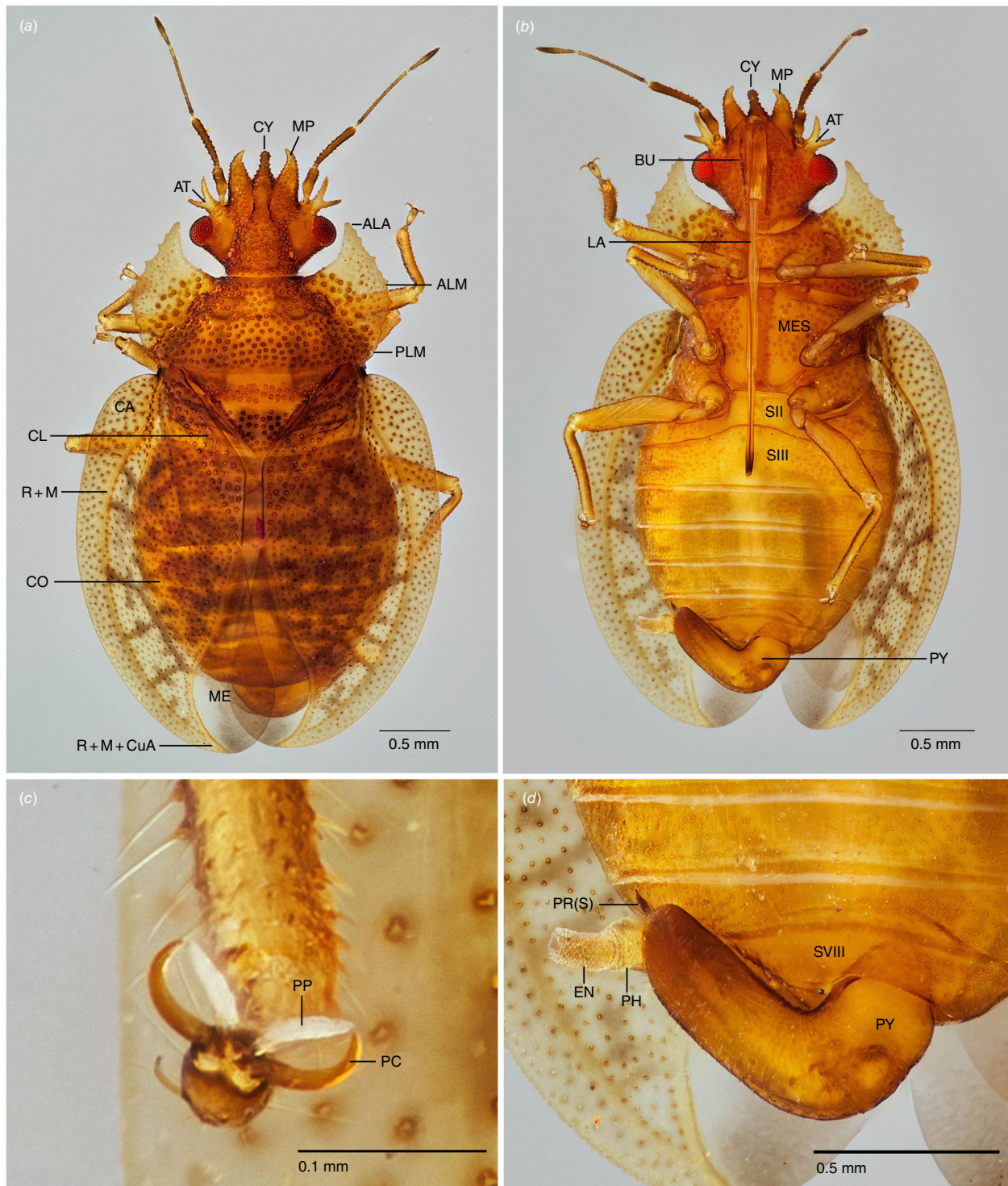


**Fig. 7.** Adult morphology of male of *Latebracoris norfolcensis* sp. nov. (a) Dorsal habitus. (b) Ventral view of body. (c) Ventral view of pretarsus of hind leg. (d) Ventral view of male pygophore, with aedeagus partly inflated. Abbreviations: ALA, anterolateral angle of pronotum; ALM, anterolateral margin of pronotum; AT, antenniferous tubercle; BU, bucculae; CA, costal area of hemelytron; CL, clavus of hemelytron; CO, corium of hemelytra; CY, clypeus; EN, endosoma of aedeagus; LA, labium; ME, hemelytral membrane; MES, mesosternum; MP, mandibular plate; PC, pretarsal claw; PH, phallosome; PLM, posterolateral margin of pronotum; PP, pseudopulvillus of pretarsus of hind leg; PR, proctiger; PR(S), proctiger spine; PY, pygophore; R + M, radius and medial vein; R + M + CuA, radius + medial + cubitus vein; SII, abdominal sternum II; SIII, abdominal sternum III; SVIII, abdominal SVIII. Scale bars as indicated.

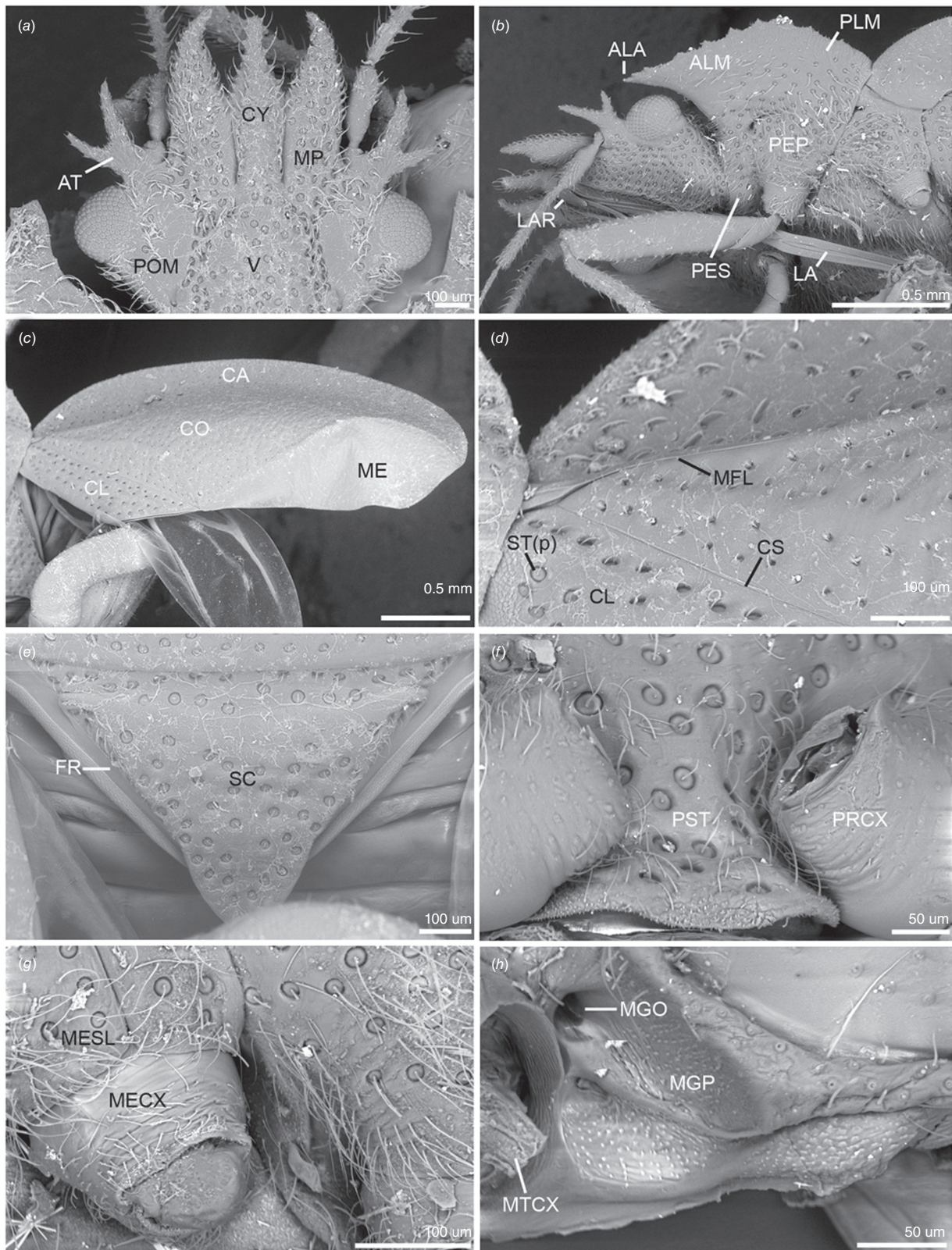


**Fig. 8.** (Caption on next page)

**Fig. 8.** Scanning electron micrographs of key head, thoracic and hemelytron characters of male of *Latebracoris norfolcensis* sp. nov. (a) Head in dorsal view. (b) Head, and pro- and mesothorax in lateral view. (c) Hemelytron in dorsal view. (d) Proximal third of hemelytron in dorsal view. (e) Scutellum and frena in dorsal view. (f) Prosternum in ventral view. (g) Propleuron in lateral view. (h) External efferent system of metathoracic gland in lateral view (pterothoracic legs removed). Abbreviations: ALA, anterolateral angle of pronotum; ALM, anterolateral margin of pronotum; AT, antenniferous tubercle; CA, costal area; CL, clavus; CO, corium; CS, claval suture; CY, clypeus; FR, frena; LA, labium; LAR, labrum; ME, hemelytral membrane; MECX, mesocoxa; MESL, meso-supracoxal lobe; MFL, median flexion line; MGO, metathoracic gland ostiole; MGP, metathoracic gland peritreme; MP, mandibular plate; MTCX, metathoracic coxa; PEP, proepimeron; PES, proepisternum; PLM, posterolateral margin of pronotum; POM, postocular margin of head in dorsal view; PRCX, procoxa; PST, prosternum; SC, scutellum; ST(p), setiferous puncture; V, vertex.

posterior margin convex, evenly rounded (Fig. 7a, b, 8b). *Scutellum*: broadly triangular, transverse, short, mostly flattened (Fig. 7a); frena elongated, subtended apically beneath apex of scutellum (Fig. 8e); mesonotum weakly exposed (Fig. 8e). *Hemelytra*: clavi prominent, short, weakly expanded distally (Fig. 7a, 8c, 10a); claval commissure reaching abdominal T5 (Fig. 7a); greatly enlarged costal region, basally with short subcostal vein; broadest proximally, apically tapering strongly, reaching tip of forewing, with 3–5 incomplete rows of setiferous tubercles (Fig. 7a, 8c, 10a); coria greatly enlarged, with short median flexion line (Fig. 7a, 8c, 10a); corium with four cells (two basal, medial and radial); hind wing with M + Cu not reaching R + SC; PCu present (Fig. 10b). *Thoracic pleura*: propleura bipartite, with horizontal ventrally facing region and shorter vertical region, with ventral margin rounded (Fig. 8b); pterothoracic pleura short, weakly convex, with pleural sutures entire (Fig. 9a). *Thoracic sterna*: prosternum hour-glass shaped, with posterior region widened (Fig. 7b, 8f); shallow labial groove extending to abdominal SIII (Fig. 7b). *Metathoracic gland*: small ostiole proximal and anterior to metacoxal cavity, projecting posterolaterally into depressed canal-like peritreme, with minute papillate dermal processes, without evaporative areas (Fig. 8h). *Legs*: coxae globose, short, widely separated, with procoxae closer to midline than pterothoracic coxae; procoxae open distinctly separated from pterothoracic coxae, paired pterothoracic coxae subcontiguous on each side (Fig. 7b, 8g, h); trochanters prominent, not fused with femora (Fig. 7b); fore and middle legs homomorphic, femora weakly expanded, tibiae cylindrical (Fig. 7b); metafemora weakly elbowed (Fig. 7b); legs with apical tibial combs (Fig. 9e); all tibiae without tibial appendix; tarsi 2-segmented, first tarsomere short, second tarsomere expanded distally,  $\sim 5\times$  longer than first tarsomere (Fig. 9e, f); pretarsus with setiform parempodia, subcontiguous; large fleshy pseudopulvilli, subequal in length to claws, attached to unguitactor plate and inner base of claws; claws evenly arcuate (Fig. 9e, f). *Abdominal venter*: broad (Fig. 7a, b); SII elongate,  $\sim 1/2$  length of SIII medially, anvil-shaped, anterior margin straight medially, sublaterally with depressions housing metacoxae; posterior margin excavate (Fig. 7b, 12b); abdominal SIII longest sternite in males, posterior margin straight (Fig. 7a); male

SIV–SVI homomorphic, margins straight (Fig. 7b); male SVI posterior margin weakly excavate (Fig. 7b); male SVII short, weakly asymmetrical, posterior margin weakly excavate (Fig. 7b, d); abdominal SVIII strongly asymmetrical, accommodating pygophore on left side (Fig. 7b, d); female abdominal terga 2–7 bilaterally symmetrical, T2 second longest tergum, T7 longest tergum, medially pinched (Fig. 12a); female venter bilaterally symmetrical, abdominal SVII longest sternum, large, apically tapered, with narrowly rounded apex (Fig. 12b); female ventrolateral tergite VIII narrowly visible in ventral view (Fig. 9c, d). *Abdominal spiracles*: ventral in position, sublateral on abdominal SII–SVII (Fig. 9a–c); female ventrolateral tergite 8 with spiracle (Fig. 9d).

Genitalia as in species description.

## Remarks

*Latebracoris* is differentiated from *Proxylastodoris* by the bifurcate v. undivided antenniferous tubercles (cf. Fig. 8a and van Doesburg *et al.* 2010, fig. 3), apically free v. contiguous mandibular plates (cf. Fig. 8a and van Doesburg *et al.* 2010, fig. 3), anterolateral angles reaching midpoint v. not reaching eyes (cf. Fig. 8a and van Doesburg *et al.* 2010, fig. 3), greatly explanate and serrated anterolateral margins v. not expanded and smooth anterolateral margins of pronotum (cf. Fig. 7a and van Doesburg *et al.* 2010, fig. 5), costal area of hemelytra broad v. narrow (cf. Fig. 7a and 10a with Doesburg *et al.* 2010, fig. 1 and 2), pygophore short v. squat (cf. Fig. 7b, d, 11a with Fig. 8a and van Doesburg *et al.* 2010, fig. 33–34), proctiger with v. without spines (cf. Fig. 11b, c with van Doesburg *et al.* 2010, fig. 33), common oviduct elongated v. short (cf. Fig. 8a and van Doesburg *et al.* 2010, fig. 3).

The monotypic genera *Latebracoris* gen. nov. and *Thaicoris* Kormilev are differentiated by the following characters: ovoid v. elongated body (cf. Fig. 7a and Heiss and Popov 2002, fig. 1), clypeus elongated and greatly surpassing mandibular plates v. subequal in length (cf. Fig. 7a, 8a and Heiss and Popov 2002, fig. 1), antenniferous tubercle reaching  $\sim 1/2$  length of mandibular plates v. subequal in length (cf. Fig. 7a, 8a and Heiss and Popov 2002, fig. 1), second antennomere  $\sim 2\times$  length of first v. subequal in length (cf. Fig. 7a and Heiss and Popov 2002, fig. 1), labium

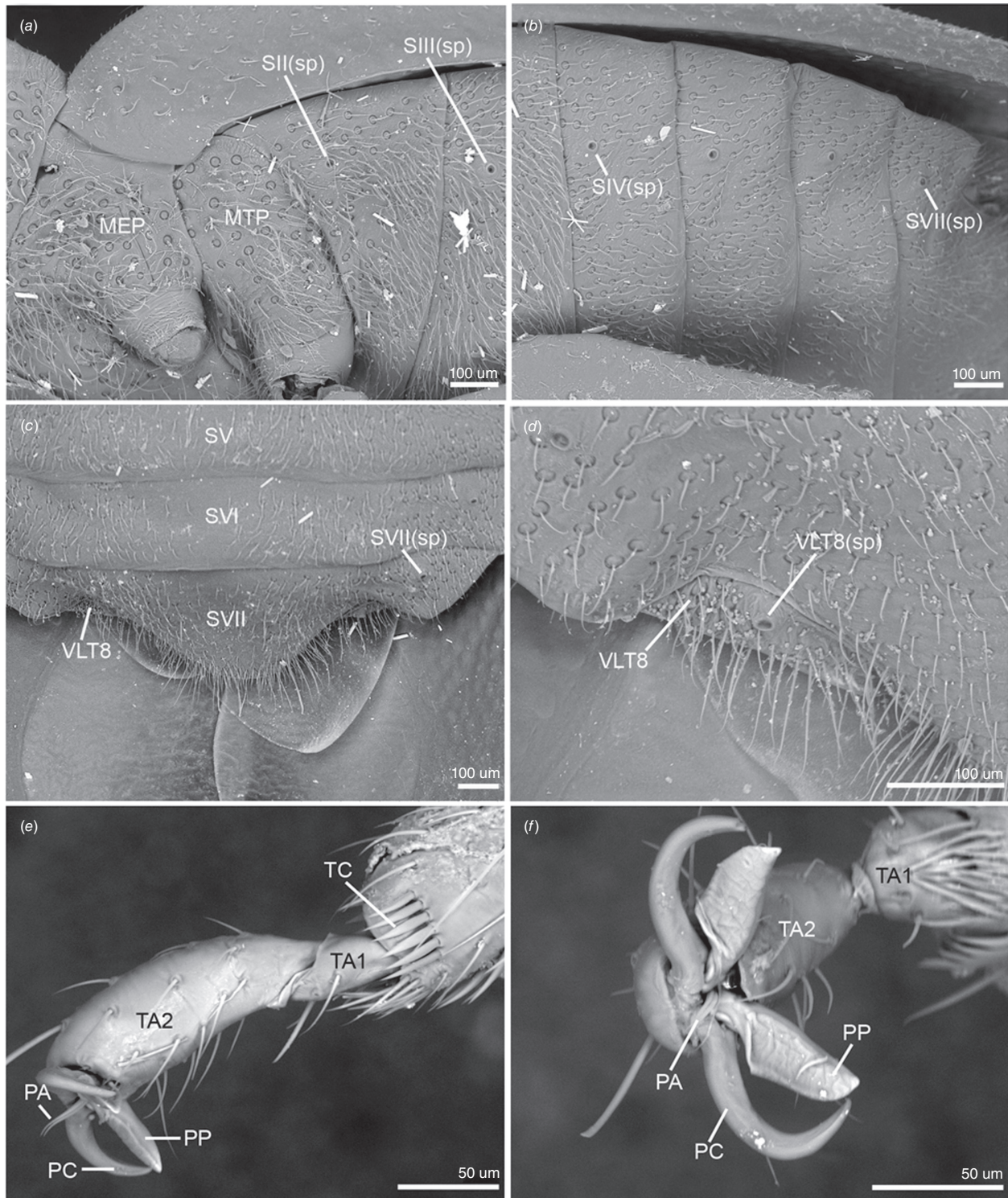


**Fig. 9.** Scanning electron micrographs of key pterothoracic, abdominal and leg characters of male of *Latebracoris norfolcensis* sp. nov. (a) Pterothoracic pleura in lateral view. (b) Abdominal venter in lateral view. (c) Abdominal apex in ventral view. (d) Ventrolateral tergite 8 and spiracle in ventral view. (e) Proleg pretarsus, tarsi and tibial apex in lateral view. (f) Proleg pretarsus in apical view. Abbreviations: MEP, mesopleuron; MTP, metapleuron; PA, parempodium; PC, pretarsal claw; PP, pseudopulvillus; SV–SVI, abdominal sterna V–VI; SII–IV(sp), abdominal sterna II–IV spiracles; SVII(sp), abdominal spiracle SVII; TA1–2, tarsomeres 1 and 2; TC, tibial comb; VLT8, ventrolateral tergite 8; VLT8(sp), ventrolateral tergite 8 spiracle.

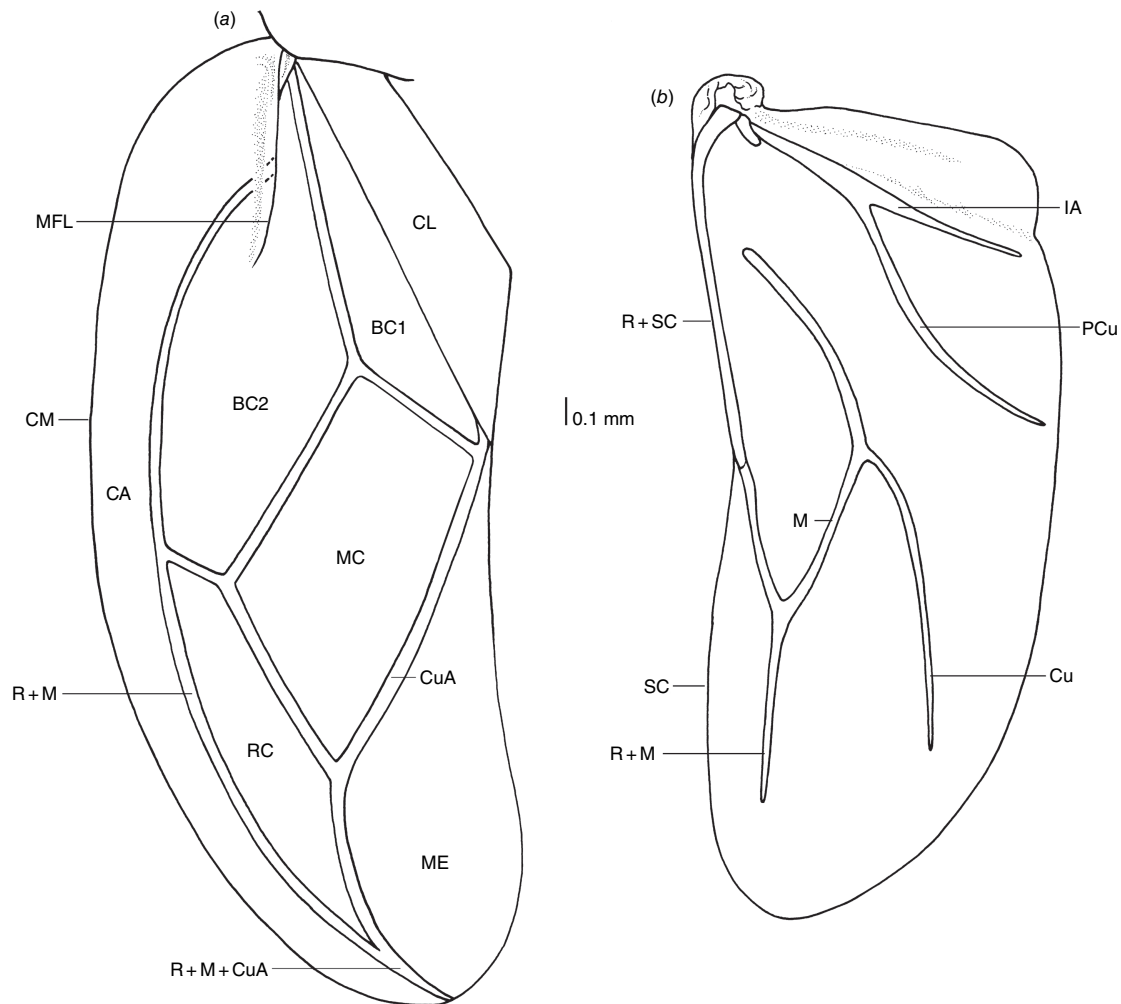


**Fig. 10.** Hemelytron and hind wing of *Latebracoris norfolcensis* sp. nov. (a) Hemelytron; (b) Hind wing. Abbreviations: BC1, first basal cell of corium; BC2, second basal cell of corium; CA, costal area; CL, clavus; CM, costal margin; CO, corium; Cu, cubitus vein; M, medial vein; M + Cu, medial + cubital vein; MC, medial cell of corium; ME, hemelytral membrane; MFL, median flexion line; PCu, post cubital vein; RC, radial cell of corium; R + M, radial + medial vein; R + M + CuA, radial + medial + cubital anterior vein; R + Sc, radial + subcostal vein; SCV, subcostal vein; IA, first anal vein.

reaching abdominal SIII v. mesosternum (cf. Fig. 7b and Heiss and Popov 2002, fig. 2), corium unpartitioned v. divided into radial, medial and distal cells (cf. Fig. 10a and Heiss and Popov 2002, fig. 1), pygophore at rest reaching abdominal SVII v. SVI (cf. Fig. 7a and Heiss and Popov 2002, fig. 1) and phallosome without elongated apical processes v. with processes (cf. Fig. 7a and Heiss and Popov 2002, fig. 2).

***Latebracoris norfolcensis* Cassis, Monteith & Postle, sp. nov.**

Norfolk Island Palm Bug

ZooBank: [urn:lsid:zoobank.org:act:D4E2BA3C-917E-4F07-96A1-E13E2C156404](https://zoobank.org/act:D4E2BA3C-917E-4F07-96A1-E13E2C156404)

**Etymology**

The species epithet is based on the restricted distribution of this species on Norfolk Island.

**Material examined (types)**

**Holotype.** NORFOLK ISLAND: ♂: -29.020°S, 167.940°E, 210 m, lower Mt Pitt Rd, 5–6 Feb 2021, Monteith & Postle, ex fruiting palm, 40341, from fruiting inflorescence of *Rhopalostylis baueri* (In QM, REG. NO. T258332). PARATYPES: 3♂3♀, same data as holotype (in QM); 1♂, same data but 8 Feb 2021, 40350 (in QM); 7♂5♀, -29.017°S, 167.946°E, 165 m, lower Palm Glen, 4 Feb 2021, Monteith & Postle, ex sprayed palm fruit, 40328 (7♂4♀ in AM and UNSW; 1♀ in QM); 6♂2♀, -29.0152°S, 167.9387°E, Mt Pitt Reserve, 14 Dec 2019, A. Postle, from fruiting inflorescence of *Rhopalostylis baueri*, 39721 (5♂2♀ in QM; 1♂ in AM); 1♂1♀, -29.016°S, 167.939°E, 260 m, lower

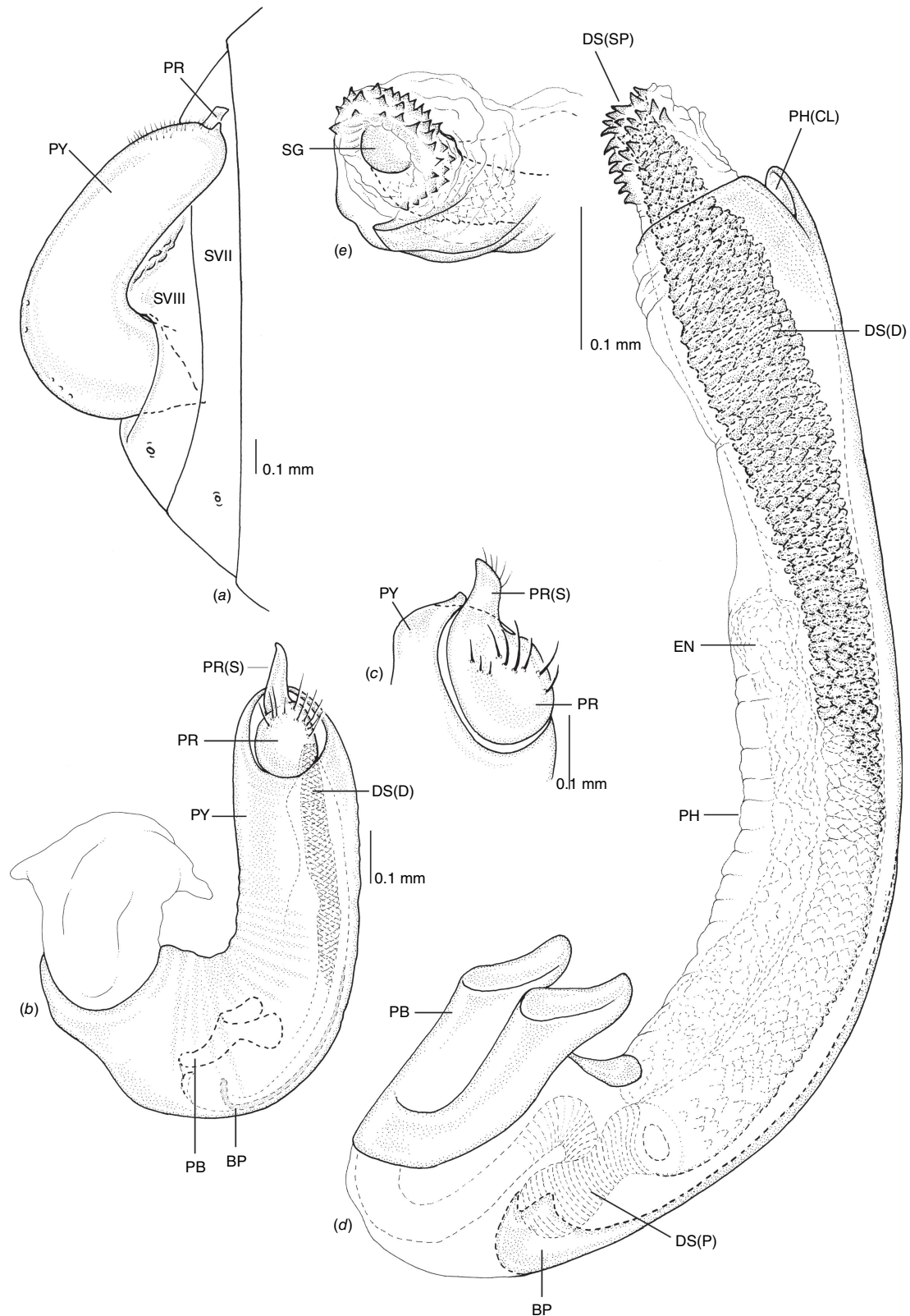


**Fig. 11.** Male genitalia of *Latebracoris norfolcensis* sp. nov. (a) Abdominal terminalia, including pygophore, ventral view. (b) Pygophore in lateral view. (c) Proctiger. (d) Aedeagus in lateral view. (e) Apex of endosoma and ductus seminis. Abbreviations: BP, basal process; DS(D), ductus seminis distalis; DS(P), ductus seminis proximalis; DS(SP), ductus seminis spines; EN, endosoma; PB, phallobase; PH, phallosome; PH(CL), phallosomal cleft; PR, proctiger; PR(S), proctiger spine; PY, pygophore; SG, secondary gonopore; SVII, SVIII, abdominal sternites VII and VIII.

Mt Bates track, 3 Feb 2021, Monteith & Postle, ex sprayed palm fruit, **40322**, from fruiting inflorescence of *Rhopalostylis baueri* (in QM); 5♂3♀, -29.014°S, 167.945°E, 205 m, upper Palm Glen, 6 Feb 2021, Monteith & Postle, spraying palm fruit **40338**, from fruiting inflorescence of *Rhopalostylis baueri* (1♂1♀ in ANIC; 1♂1♀ in AMNH; 1♂1♀ in NHM; 2♂ in QM); 3♂4♀, -29.016°S, 167.938°E, 265 m, lower Mt Bates track, 3 Feb 2021, Monteith & Postle, ex sprayed palm fruit. **40323**, from fruiting inflorescence of *Rhopalostylis baueri* (in QM, MNHN); 1♀, -29.0117°S, 167.9536°E, McLachlans Lane, NINP, 115 m, 17.ix.2022, J.M.H. Tweed, beaten from green palm berries from fruiting inflorescence of *Rhopalostylis baueri* (in QM).

### Other material examined (Non-types)

NORFOLK ISLAND: 1♀ 3 nymphs, data as for sample **40323** above (DNA quality specimens in UNSW); 1♀, data as for sample **40341** above (DNA quality specimen in AM); 140 nymphs, data as for sample **40328** above (in QM and AM); 6 nymphs and eggs on palm fruit bracts, data as for sample **40322** above (in QM, AM and UNSW); 25 nymphs, data as for sample **40338** above (in QM); 76 nymphs, data as for sample **40323** above (in QM); eggs on palm fruit bracts, data as for sample **40341** above (in QM); Eggs on palm fruit bracts, -29.016°S, 167.939°E, 260 m, lower Mt Bates track, 5 Feb 2021, Monteith & Postle, **40333** (in QM).

### Diagnosis

*Latebracoris norfolcensis* is recognised by the following combination of characters: body dark greyish-brown in life (Fig. 3a–d), pale yellowish-brown in ethanol preserved specimens, with translucent lateral margins of pronotum and costal region of hemelytra (Fig. 7a); body with dense distribution of setiferous punctures (Fig. 7a, b, 8d), each with a single hair-like seta; first and second antennomeres and lateral margins of head with setiferous tubercles (Fig. 7a); pygophore geniculate, tubiform in outline (Fig. 11a, b); proctiger cap-like, with spine (Fig. 11c); parameres absent (Fig. 11c); ductus seminis proximalis narrowly annulated (Fig. 11d); ductus seminis distalis with tile-like texture (Fig. 11d); endosoma with scythe-like sclerotised basal process (Fig. 11d); common oviduct elongated and annulated (Fig. 12c); lateral oviducts short and annulated, with enlarged round reservoirs (Fig. 12c).

### Description

#### Colouration

Body and appendages mostly dark greyish-brown in life (Fig. 3a–d), light orangish-brown in preserved specimens, with lateral regions of pronotum and costal region translucent; corium often with anastomising dark brown highlighting (Fig. 7a, b); antennae often darker brown (Fig. 7a, b).

#### Vestiture and texture

Body with dense distribution of setiferous punctures, with each puncture housing a hair-like seta on a tubercle (Fig. 7a, b, 8d); punctures densely distributed on head, pronotum, scutellum, hemelytra, thoracic pleura and sterna

(e.g. Fig. 8f), shallower and densely distributed on abdominal venter (e.g. Fig. 7b).

### Male genitalia

Pygophore as a geniculate tube, oval in cross-section, mostly straight, narrow, inserted on left side of body (Fig. 7b, d, 11b, d); proctiger cap-like, with spine (Fig. 7b, 11b, c); parameres absent (Fig. 11b, c); aedeagus tubular, inserted for full length of pygophore (Fig. 11b), elongated, arcuate (Fig. 11d); phallosome with apical cleft (Fig. 11d); endosoma membranous, medially attached to phallosome, apically with spinule-shaped sclerotisation adjacent to secondary gonopore (Fig. 11d, e); ductus seminis proximalis tubular with annulated outer wall (Fig. 11d), ductus seminis distalis elongate, with tile-like texture (Fig. 11d); secondary gonopore simple, round (Fig. 11d, e).

### Female genitalia

Bursa copulatrix membranous, pouch-like, subtriangular shaped, tapering caudally, without sclerotisation (Fig. 12c); common oviduct annulated, elongated, with short annulated lateral oviducts with round reservoir-like structures, proximal to junction with common oviduct (Fig. 12c).

### Measurements

**Males.** Mean body length 4.53 ( $n = 10$ ), range 4.33–4.83, mean body width 2.71, range 2.52–2.84.

**Females.** Mean body length 4.66 ( $n = 9$ ), range 4.45–4.86; mean body width 2.77, range 2.71–2.81.

**Holotype male.** Body length 4.36; maximal abdominal width 2.71; hemelytra length 3.00; hemelytra width 1.36; head length 0.80; head width across eyes 1.07; head width between eyes, 0.76; eye width 0.15; width between ocelli, 0.40; ocelli diameter 0.03; antennomeres: total length 1.46; I 0.21, II 0.43, III 0.55, IV 0.27; rostrum: total length 2.30; I 0.45; II 0.55; III 0.63; IV 0.69; pronotal length 0.76; maximal pronotal width 2.00; anterior pronotal width 1.24; scutellum length 0.70; scutellum width 1.17.

### Remarks

*Latebracoris norfolcensis* is differentiated from *Thaicoris sedlaceki* and *Proxylastodoris kuscheli* by non-genitalic differences as provided in the *Latebracoris* generic remarks section, including the shape of the head and pronotum (Fig. 7a, 8a). *Latebracoris norfolcensis* is unequivocally separated from *P. kuscheli* by the male genitalia, including the following character states: proctiger with a spine v. not spinose (cf. Fig. 11b, c and van Doesburg *et al.* 2010, fig. 33), pygophore elongated v. squat (cf. Fig. 8d, 11b, c and van Doesburg *et al.* 2010, fig. 33), ductus seminis distalis elongated and tile-like v. short and tubular (cf. Fig. 11c and van Doesburg *et al.* 2010, fig. 33), and common oviduct elongated v. short (cf. Fig. 12c and van Doesburg *et al.* 2010, fig. 32).

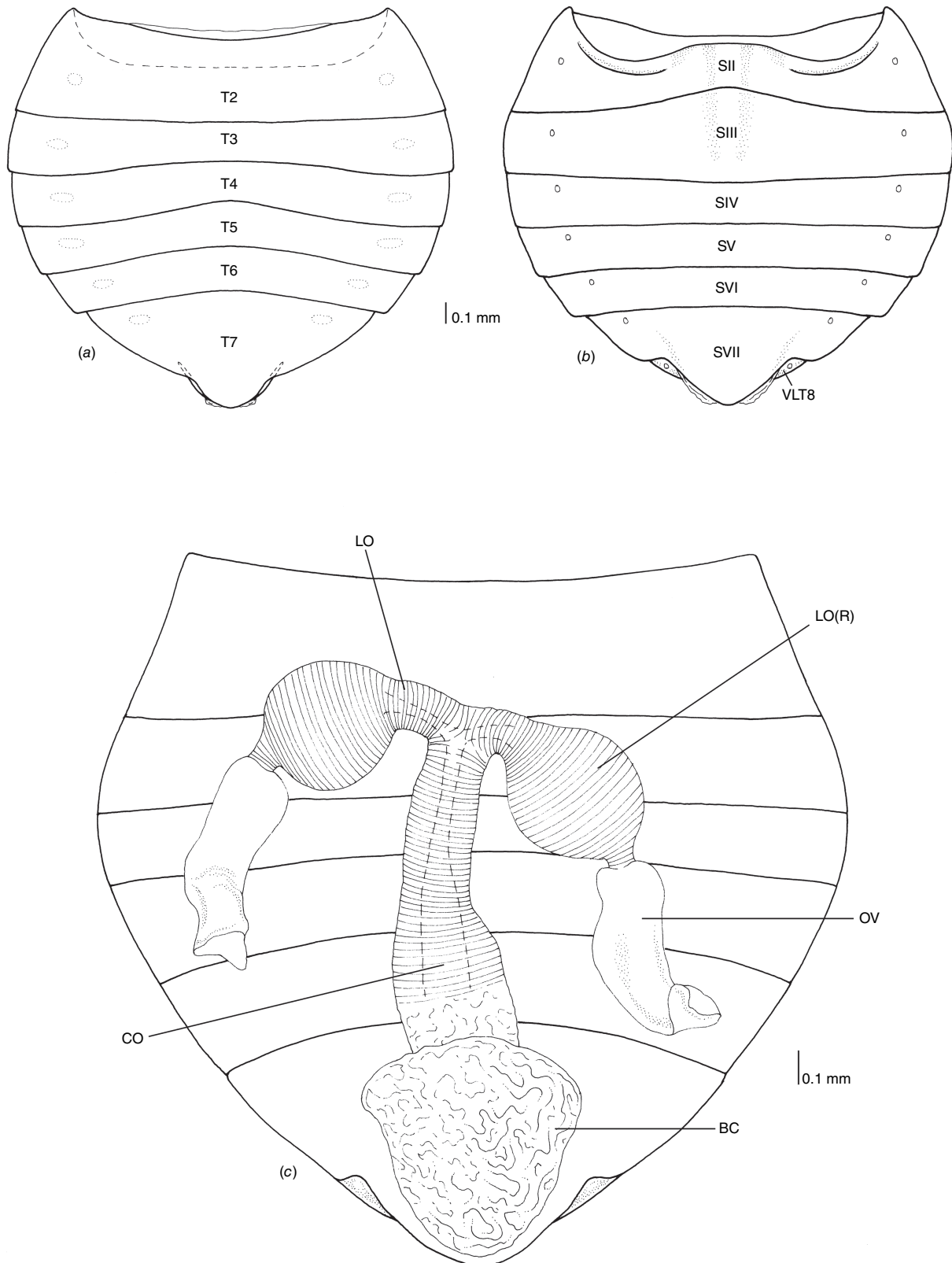


**Fig. 12.** Female genitalia of *Latebracoris norfolcensis* sp. nov. (a) Abdomen in dorsal view. (b) Abdominal venter. (c) Bursa copulatrix, oviducts and ovarioles. Abbreviations: BC, bursa copulatrix; CO, common oviduct; LO, lateral oviduct; LO(R), lateral oviduct reservoir; OV, ovariole; SII–SVII, abdominal sterna 2–7; T2–T7, abdominal terga 2–7; VLT8, ventrolateral tergite 8.

Heiss and Popov (2002) provided few details of the male genitalia of *Thaicoris sedlaceki* and there is no information on the female genitalia. Based on the illustration, the pygophore is more elongated overall and has an elongated apical spur, differentiating this from that of *L. norfolcensis* that is shorter and lacking an elongated apical spur (cf. Fig. 11a–c and Heiss and Popov 2002, fig. 3–5). Also, the proctiger spine in *L. norfolcensis* is not present in *T. sedlaceki*.

## Phylogeny

### Characters and character states

The characters and character states are as described below, with commentary where definitions are required or alternative hypotheses exist. References to figure numbers are from published works and are provided as evidence of character states codified herein, and figure numbers cited for *Latebracoris norfolcensis*. The data matrix is given in Table 1.

**Character 0. Body depression: 0 – not flattened; 1 – flattened.** This is defined by both surfaces flattened, compared to the ventral surface in most cimicomorphans being convex in profile. The flattened state is present in most Xylastodorinae (not *Proxylastodoris* spp.) and the thaumastocorine genera *Baclozygum* and *Thaumastocoris* (e.g. Noack *et al.* 2011, fig. 12E). The abdominal venter in the thaumastocorine genus *Onymocoris* is convex and the body is codified as not flattened (e.g. Cassis *et al.* 1999, fig. 15).

**Character 1. Hemelytral texture: 0 – smooth; 1 – punctate; 2 – aerolate; 3 – setiferous punctures (setae short); 4 – setiferous punctures (setae long).** The hemelytral texture varies considerably in the Miroidea, from smooth as in most species of Miridae (e.g. Sanchez and Cassis 2018, fig. 8A), aerolate as in most Tingidae (e.g. Cassis and Symonds 2008, fig. 9E), to having setiferous punctures in the Thaumastocoridae (e.g. Fig. 8d, ST(p)).

**Character 2. Cephalic spines: 0 – absent; 1 – present.** Cephalic spines are characteristic of most Tingidae, with most taxa having at least five spines as in the Tinginae: Tingini (e.g. Cassis and Symonds 2008, fig. 9A); these are not present in the Vianaidinae. In some Tingini genera, with greatly reduced somatic characters, the cephalic spines are near obsolete, as in species of the Australian genus *Malandiola* Horváth, 1925, where secondary loss is likely.

**Character 3. Mandibular plates position: 0 – lateral; 1 – dorsal.** The dorsal character state is found in the Thaumastocoridae, where the mandibular plates and antennifers have become dorsalised, particularly in *Thaumastocoris* (e.g. Noack *et al.* 2011, fig. 15A) and *Discocoris* (Slater and Schuh 1990, fig. 1). In most Miridae the mandibular plates are

wholly in the lateral position (e.g. Cassis and Symonds 2016, fig. 28B). The mandibular plate Character 2 in Schuh and Štys (1991) and Character 3 in Schuh *et al.* (2009) are in part encapsulated in Characters 4–8 in this analysis

**Character 4. Mandibular plates dorsal profile: 0 – convex; 1 – flat to concave.** In Thaumastocoridae the mandibular plates can be either flat or concave in *Thaumastocoris* (e.g. Noack *et al.* 2011, fig. 15A) and *Discocoris* (e.g. Slater and Schuh 1990, fig. 1) or round as in *Baclozygum* and *Onymocoris* (e.g. Cassis *et al.* 1999, fig. 2). This is also apparent in the fossil xylastodorine *Paleodoris lattini* (Poinar and Santiago-Blay 1997, fig. 1 and 2).

**Character 5. Mandibular plates length cf. clypeus length: 0 – shorter than clypeus; 1 – subequal to clypeus; 2 – longer than clypeus.** In Miroidea the length of the mandibular plates varies from short to significantly surpassing the clypeus, with the latter often the case in thaumastocorids with flattened mandibular plates (see Character 4 for figure citations).

**Character 6. Mandibular plates apically: 0 – separated; 1 – contiguous.** Where the mandibular plates extend beyond the clypeus in the Thaumastocoridae, these are either separated as in *Baclozygum depressum* (Drake and Slater 1957, fig. 1) or contiguous beyond the clypeus as in *Discocoris* spp. (e.g. Slater and Schuh 1990, fig. 1).

**Character 7. Mandibular plates and clypeus lateral connection: 0 – contiguous; 1 – separated.** The separated state is homologous for *Latebracoris norfolcensis* (Fig. 7a) and *Thaicoris sedlaceki* (e.g. Heiss and Popov 2002, fig. 1).

**Character 8. Antenniferous tubercles: 0 – absent; 1 – present, short; 2 – short, thorn-like; 3 – present, large.** Processes associated with the antennifers are pronounced in the Xylastodorinae, particularly in *Latebracoris norfolcensis* (Fig. 7a) and *Paleodoris lattini* (Poinar and Santiago-Blay 1997, fig. 1 and 2). These are also present in most Tingidae (Cantacaderinae, Tinginae) although their homology with those in the Xylastodorinae is questionable. Antenniferous tubercles are not present in either the Thaumastocorinae or Vianaidinae.

**Character 9. Preocular region laterally: 0 – not thick and round; 1 – thick and round.** The preocular region of the Thaumastocorinae is typically convex in outline and thickly rounded in profile (e.g. Noack *et al.* 2011, fig. 15A), and is differentiated from the shorter and less arcuate preocular margin found in the Xylastodorinae (e.g. van Doesburg *et al.* 2010, fig. 3).

**Character 10. Clypeus shape: 0 – not spindle shaped; 1 – spindle shaped.** The spindle condition is homologous for *Latebracoris norfolcensis* (Fig. 7a) and *Paleodoris lattini*





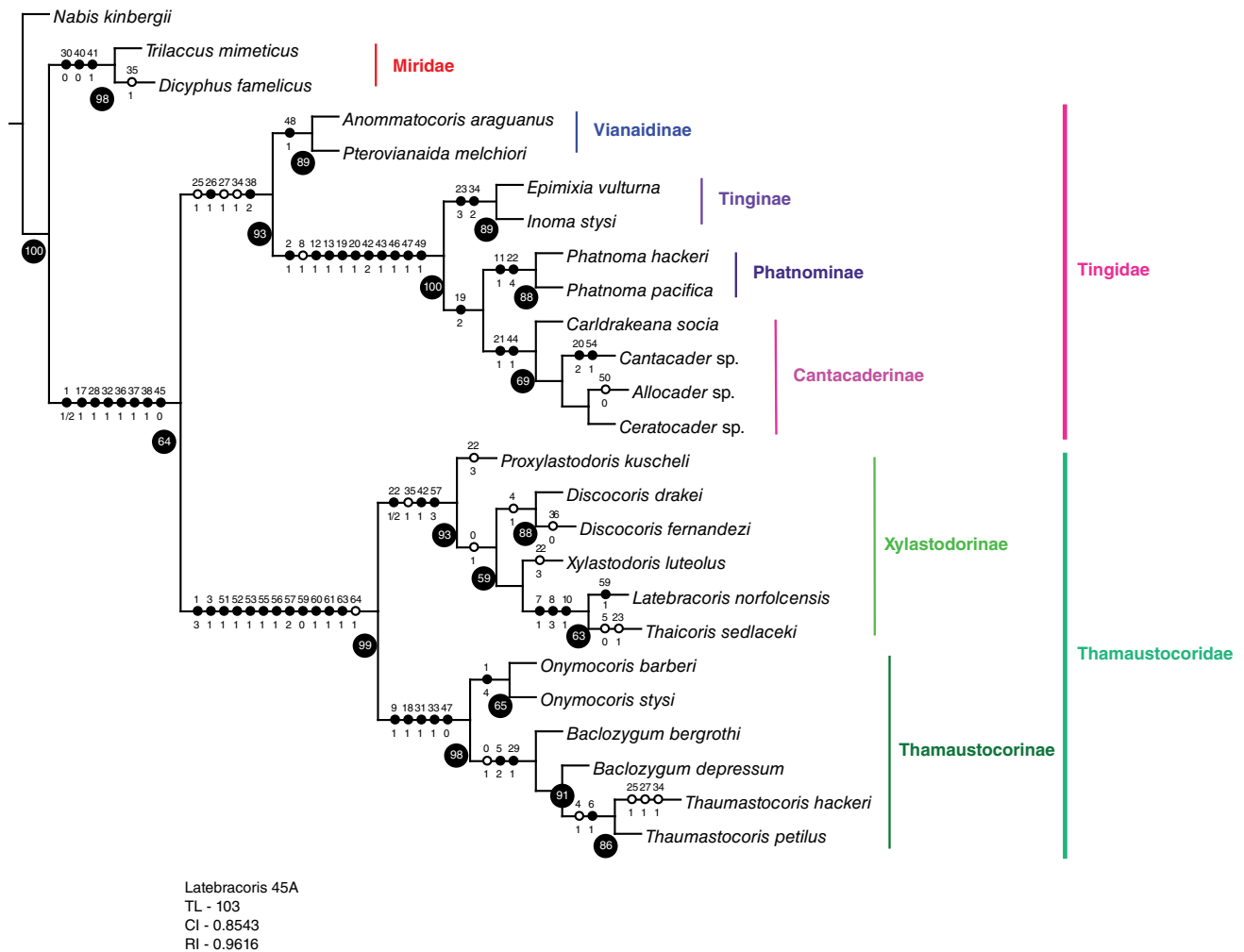


**Fig. 13.** Implied weights phylogeny of Miroidea of Recent taxa. Character state transformations are given for each node or on branches to terminal taxa. Uncontradicted synapomorphies are closed circles, with character number above and character state below each circle. Contradicted synapomorphies are given in open circles, including on branches to terminal taxa. Resampling values > 50% are given in black circles at nodes.

(Poinar and Santiago-Blay 1997, fig. 1 and 2), and is unlike any other described fossil or Recent thaumastocorid.

**Character 11. Clypeal spine presence: 0 – absent; 1 – present.** The presence of a clypeal spine (Lis 1999, fig. 16) was posited as a synapomorphy for the Phatnominae by Lis (1999) and was observed as such for the two *Phatnoma* species in this analysis. Lis (1999) raised the Phatnominae to subfamilial rank on the basis of this character.

**Character 12. Bucculae anterior position (ventral view): 0 – not exceeding clypeus; 1 – exceeding clypeus.** The anteriorly extended bucculae that reach beyond the clypeus is a character common in the Tinginae (e.g. Cassis and Symonds 2008, fig. 9B) and Cantacaderinae (Lis 1999, fig. 14) but not the Vianaidinae (Schuh et al.

2006, fig. 4A, B). The bucculae do not extend as such in the Thaumastocoridae (Fig. 8b).

**Character 13. Bucculae posterior position: 0 – not reaching prosternum; 1 – reaching prosternum.** The bucculae typically extend to the prosternum in most Tingidae (e.g. Cassis and Symonds 2008, fig. 9B), aside from the Vianaidinae that reach near the posterior margin of the head (Schuh et al. 2006, fig. 4C). Bucculae are short in the thaumastocorids, as in the genus *Thaumastocoris* (e.g. Noack et al. 2010, fig. 15B).

**Character 14. Ocelli: 0 – absent; 1 – present.** The presence of ocelli is universal in the Thaumastocoridae, as in *Latebracoris norfolcensis* (Fig. 7a) and these are in a postocular position. In contrast to other Miroidea, ocelli

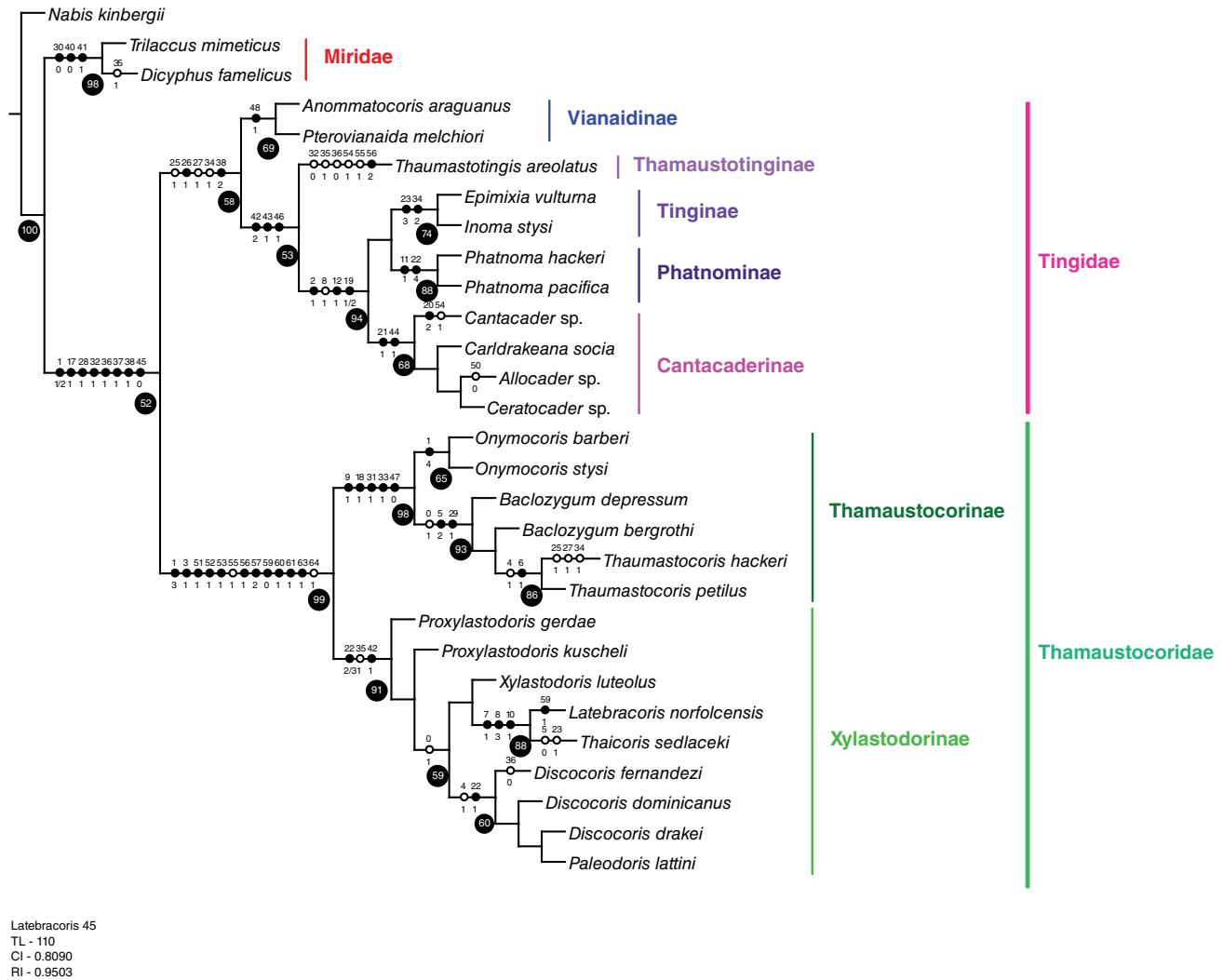


**Fig. 14.** Implied weights phylogeny of Recent and fossil taxa of Miroidea. Character state transformations are given for each node or on branches to terminal taxa. Uncontradicted synapomorphies are closed circles, with character number above and character state below each circle. Contradicted synapomorphies are given in open circles, including on branches to terminal taxa. Resampling values >50% are given in black circles at nodes.

are absent in all Tingidae and Miridae aside from the subfamily Isometopinae (Schuh 1976; Cassis and Schuh 2012).

**Character 15. Labium insertion: 0 – anterior; 1 – ventral.** The point of cephalic insertion of the labium distinguishes the predaceous (anterior), as in *Nabis kinbergii*, from the herbivorous (ventral) lineages in the Cimicomorpha (Schuh and Štys 1991; Schuh et al. 2006). The ventral state is universal for the Miroidea, including in *Latebracoris norfolcensis* (Fig. 7b).

**Character 16. Labium profile: 0 – curved; 1 – straight, parallel to body.** The labium in profile is also characteristic of herbivorous lineages, being horizontal and parallel to the body, including all Miroidea (e.g. Schuh et al. 2006,

fig. 4E). The curved state is in the predaceous outgroup species *Nabis kinbergii*.

**Character 17. Apex of mandibular stylets: 0 – with teeth or pointed ridges; 1 – with rounded transverse elevations.** This character was recognised by Schuh et al. (2009) as phylogenetically significant in the Cimicomorpha, and shared between the Thaumastocoridae and Tingidae. Schuh et al. (2009) based this primarily on the observations of Cobben (1978). We did not observe this character and have codified this as in Schuh et al. (2009).

**Character 18. First labial segment: 0 – elongate, narrow; 1 – short, dilated.** The short and dilated first labial segment is homologous in the Thaumastocoridae. Schuh and

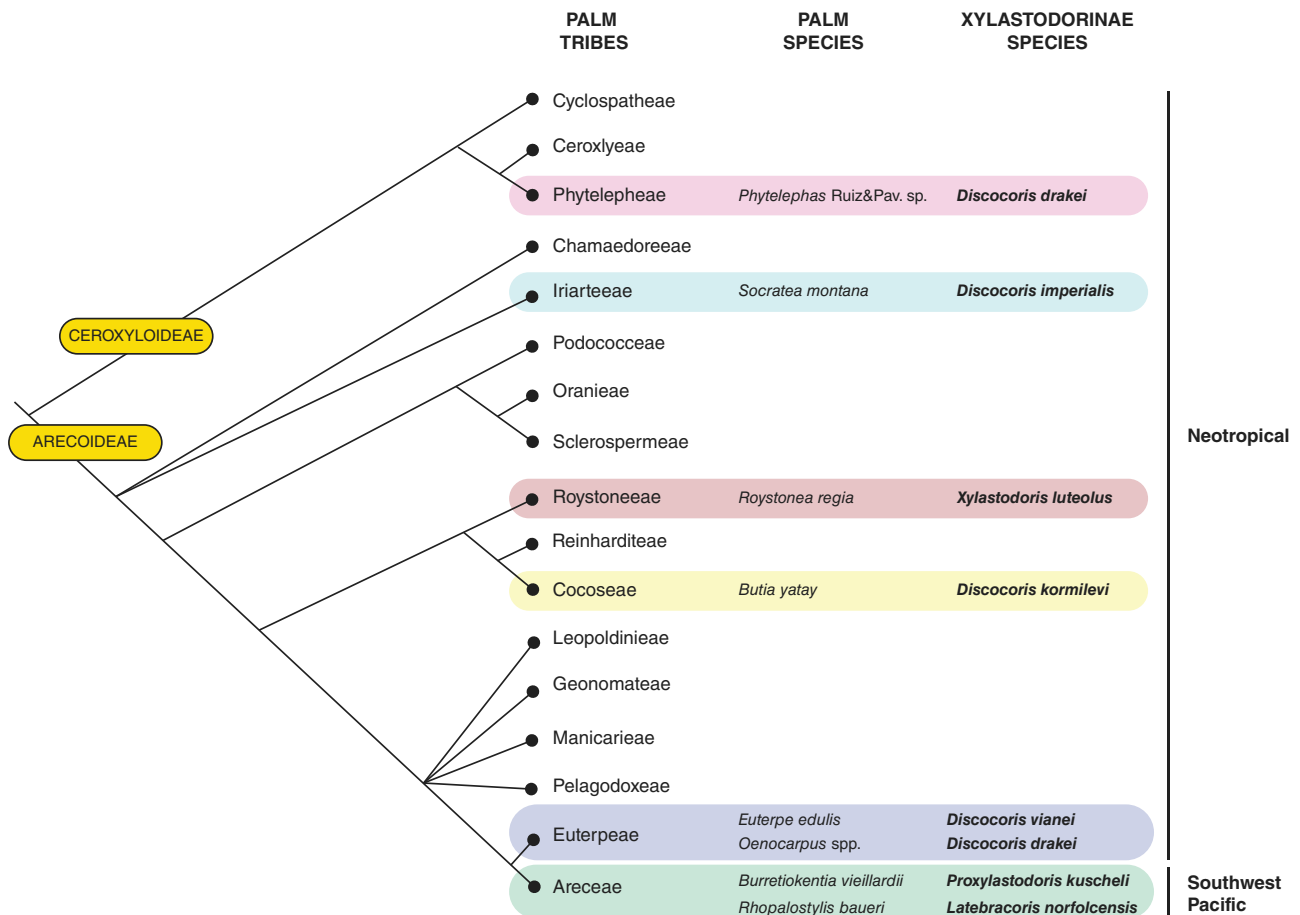


**Fig. 15.** Mapping of palm association data for all known Xylastodorinae species to an abridged palm tribal phylogeny (not including Calamoideae, Nypoideae and Coryphoideae) redrawn from Baker and Dransfield (2016). *Oenocarpus* species given in full in Table 2.

Štys (1991) codified Tingidae as having a dilated first labial segment (e.g. Noack et al. 2011, fig. 14B). We did not observe this in the Tingidae (e.g. Cassis and Symonds 2008, fig. 9B) nor the Xylastodorinae (e.g. Fig. 8b).

**Character 19. Antennae AI and AII relative lengths: 0 – All much longer than AI; 1 – subequal in length; 2 – All shorter or subequal to AI.** States 2 and 3 are characteristic of the Tingidae aside from the Vianaidinae, corroborating the observations of Lis (1999).

**Character 20. Pronotal carinae: 0 – absent; 1 – one to three; 2 – five.** Drake and Davis (1960) documented the presence of pronotal carinae in the Tingidae. Lis (1999) codified this character in a phylogenetic analysis, that distinguishes Tingidae from other miroids.

**Character 21. Lateral carinae on pronotal collar: 0 – absent; 1 – present.** Character state 1 is diagnostic for the Cantacaderinae (Lis 1999).

**Character 22. Anterolateral angles of pronotum: 0 – not projected anteriorly; 1 – greatly projected anteriorly, apex rounded without areolation; 2 – greatly projected anteriorly, apex acute without areolation; 3 – short, with acute angle or forward projecting tubercle; 4 – strongly projected anteriorly, deeply serrate.** The greatly projected anterolateral angles of the pronotum are diagnostic for most xylastodorine species, aside from *Proxylastodoris* spp. (e.g. van Doesburg et al. 2010, fig. 1) and *Xylastodoris luteolus* (Schuh and Slater 1995, fig. 52.2A) that have a small forwardly projected angle or tubercle. The greatly projected anterolateral angles may be apically rounded (e.g. Slater and Schuh 1990, fig. 1) or acute as in *Latebracoris norfolcensis* (Fig. 7a), with both lacking areolation. The projected state is also present in *Phatnoma* spp. (e.g. Lis 1999, fig. 52), with serration. The greatly projected state is correlated with the head deeply embedded into the pronotum.

**Character 23. Posterior margin of pronotum: 0 – straight; 1 – excavated; 2 – convex (incl. medially); 3 – triangular plate.** Character state 3 is diagnostic for the

Tinginae (Schuh and Štys 1991; Lis 1999; Cassis *et al.* 2019, fig. 51D). Character state 2 refers to that found in *Thaicoris sedlaceki* (e.g. Heiss and Popov 2002, fig. 1).

**Character 24. Scutellum exposed: 0 – without tubercle; 1 – with tubercle.** This character primarily pertains to Tingidae ingroup relationships and the presence of the scutellar tubercle (e.g. Lis 1999, fig. 42–45) is coupled with Character state 23-0.

**Character 25. Prosternum sulcation: 0 – flat to weakly sulcate; 1 – sulcate.** The thoracic sterna in the Miroidea are distinctive in the Tingidae (Drake and Davis 1960), where the prosternum is sulcate (e.g. Cassis *et al.* 1999, fig. 54B), including the Vianaidinae (e.g. Schuh *et al.* 2006, fig. 54A).

**Character 26. Prosternal margins: 0 – not laminate; 1 – laminate; 2 – carinate.** The prosternal margins are laminate in the Tingidae. See figure citations in Character 25.

**Character 27. Pterothoracic sternal margins: 0 – flat; 1 – laminate.** The pterothoracic margins are also laminate in the Tingidae. See figure citations in Character 25.

**Character 28. Coxae shape: 0 – conical elongated; 1 – globose.** The coxae are globose in Tingidae (e.g. Cassis *et al.* 2019, fig. 33C) and Thaumastocoridae (Fig. 7b), differentiating these from Miridae that have at least the procoxae elongated, as well as in the Nabidae.

**Character 29. Procoxae: 0 – open; 1 – closed.** In the thaumastocorine genera *Baclozygum* and *Thaumastocoris* the procoxae are closed off posteriorly by an extension of the proepimeron (Noack *et al.* 2011, fig. 13B). These are open in *Onymocoris* and the Xylastodorinae as in *Latebracoris norfolcensis* (Fig. 8f).

**Character 30. Femoral trichobothria: 0 – present; 1 – absent.** Femoral trichobothria are diagnostic for the Miridae (Schuh 1976; Cassis and Schuh 2012) and are not present in Tingidae and Thaumastocoridae.

**Character 31. Tibial appendix type: 0 – absent; 1 – present.** The tibial appendix is codified as unique to the Thaumastocorinae (e.g. Noack *et al.* 2011, fig. 12F). Weirauch (2007) proposed homology of fossula spongiosa in the Cimicomorpha, though acknowledging the possibility of independent origins between the Nabidae and Thaumastocoridae. The recognition of a fossula spongiosa in *Proxylastodoris* by van Doesburg *et al.* (2010) was not clearly formulated and the grouping of setae at the tibial appendix in *P. kuscheli* is not considered homologous with that in the Thaumastocorinae (see discussion) herein. More

broadly, the fossula spongiosa is likely non-homologous as applied to the Cimicomorpha (Weirauch 2007) and requires further investigation.

**Character 32. Tarsal number: 0 – three segmented; 1 – two segmented.** Two-segmented tarsi are diagnostic for the Tingidae and Thaumastocoridae. The fossil taxon *Thaumastotisingis areolatus* has three segmented tarsi (Heiss and Popov 2002), unlike other tingids or thaumastocorids. In the Miridae tarsi are three segmented aside from the Isometopinae (Schuh 1976; Cassis and Schuh 2012).

**Character 33. Tarsal development: 0 – well developed; 1 – greatly reduced.** All Thaumastocorinae species have greatly reduced tarsi, reminiscent of burrowing Cydnidae, with reduction in the thaumastocorines coupled with the presence of the tibial appendix (e.g. Noack *et al.* 2011, fig. 12F).

**Character 34. Parempodial type: 0 – elongated setiform (longer than parempodial sclerite); 1 – short setiform (subequal to parempodial sclerite); 2 – scale-like.** Schuh (1976) defined pretarsal structures in the Miridae, including the parempodia. Schuh *et al.* (2006) documented the reduced and scale-like parempodia in the Tingidae, inclusive of the Vianaidinae (Schuh *et al.* 2006, fig. 7A–F).

**Character 35. Pseudopulvilli: 0 – absent; 1 – present.** Pseudopulvilli are characteristic of all Xylastodorinae, as in *Latebracoris norfolcensis* (e.g. Fig. 7c, 9g) and are rejected as pulvilli, based on the attachment to both the unguitactor plate and base of claws *sensu* Schuh (1976) (van Doesburg *et al.* 2010). Fleshy pretarsal structures, termed pulvilli, are also present in other cimicomorphans (e.g. Anthocoridae: Oriini) (Schuh and Slater 1995) and fossils such as *Thaumastotisingis areolatus* (Heiss and Popov 2002). This indicates independent origins given its occasional and unrelated occurrence in the Cimicomorpha aside from the Miridae (latter attached to ventral surface of claws, see Schuh 1976).

**Character 36. Apex of terminal tarsus: 0 – without linguiform process; 1 – with linguiform process.** The presence of a linguiform process is common in the Tingidae (Cassis *et al.* 2019, fig. 49A) and Thaumastocoridae (van Doesburg *et al.* 2010, fig. 24 and 25). This is a narrow flange-like medial process on the apex of the second tarsomere, that projects over the unguitactor plate.

**Character 37. Dorsal arolium: 0 – reduced, as small bump; 1 – absent.** Schuh *et al.* (2009) codified the character states of the dorsal arolium in the Heteroptera. In this analysis we reduced the character states to two, differentiating those that are without a dorsal arolium as in the Tingidae (Schuh *et al.* 2006, fig. 7E) and Thaumastocoridae (Fig. 9f) from the Miridae where this is reduced to a bump (e.g. Schuh *et al.* 2009, fig. 3F).

**Character 38. Median flexion line of hemelytra:** 0 – elongated; 1 – short; 2 – obsolete. The median flexion line is a character used in the classification of the Miridae, where it is generally long ( $> \frac{1}{2}$  length of the corium) (Cassis 1995). This line is also recognised in the Xylastodorinae, where short and basally adjacent to R + M as in *Latebracoris norfolcensis* (Fig. 8c). This is also apparent in the Thaumastocorinae, adjacent to the costal margin (e.g. Noack et al. 2011, fig. 3A). We found no evidence of a median flexion line in the Tingidae.

**Character 39. Corium length:** 0 –  $\frac{2}{3}$  length of hemelytron; 1 – near hemelytron tip. In the Miroidea, the elongated corium is present in the Tingidae and the Xylastodorinae as in *Latebracoris norfolcensis* (e.g. Fig. 7a, 10a). The corium in the Thaumastocorinae is not elongated, and is  $\sim 2/3$  length of the hemelytra (Noack et al. 2011, fig. 7d).

**Character 40. Costal fracture:** 0 – present; 1 – absent. The costal fracture is only present in the Miridae amongst the other families of the superfamily Miroidea (Schuh et al. 2006, 2009; Weirauch et al. 2019).

**Character 41. Cuneus:** 0 – absent; 1 – present. The presence of a cuneus is contingent on the presence of a costal fracture. The cuneus is present in numerous cimicomorphan families (incl. Joppeicidae, Miridae, Microphysidae and cimicoid families). In the Miroidea this is only found in the Miridae (Cassis and Schuh 2012; Schuh and Weirauch 2020).

**Character 42. Costal area/embolium:** 0 – narrow to carinate; 1 – explanate, not areolate; 2 – explanate, areolate. We identify the first area between the costal margin and the first recognisable vein, as either the costal area (Tingidae) (e.g. Cassis et al. 2019, fig. 10E) or embolium as in the Miridae (Schuh and Slater 1995, fig. 10.1). The character states refer to costal area width and texture (e.g. areolate). See discussion section below for further evaluation.

**Character 43. Subcostal area:** 0 – absent; 1 – present. In this analysis, the subcostal area is present in the Tingidae (as in Cassis and Symonds 2008, fig. 4E), including in macropterous Vianaidinae, as in *Anommatocoris bolivianus* Schuh, Cassis, Guilbert 2006 (Schuh et al. 2006, fig. 1A).

**Character 44. Stenocostal area:** 0 – absent; 1 – present. Lis (1999) codified the stenocostal area as diagnostic of the Cantacaderinae that is anterior to the costal area (Froeschner 1996, fig. 1).

**Character 45. Hemelytral membrane:** 0 – lacking veins or cells; 1 – one or two closed cells; 2 – closed basal cells with radiating veins. Unlike the Miridae, the other taxa in

this analysis lack veins or cells (not to be confused with areolation as in Tingidae).

**Character 46. Hemelytral membrane texture:** 0 – not aerolate; 1 – areolate (at least in part). Although, lacking hemelytral membrane veins, the hemelytra in Tingidae are typically fully areolate (Tinginae) or at least in major part, with the remainder sometimes narrowly membranous (Cantacaderinae) (Lis 1999, fig. 47). This is posterior to the cubital vein and positionally homologous to the membrane of the Miridae and Thaumastocoridae.

**Character 47. Metathoracic gland external efferent system:** 0 – absent; 1 – present, anterior; 2 – present, posterior; 3 – present, medial. The metathoracic gland external efferent system is present in most taxa in the Miroidea, aside from the Thaumastocorinae (Drake and Slater 1957; Schuh and Slater 1995) and secondary losses in the Miridae (e.g. Cassis and Schuh 2012, loss in Monaloniini).

**Character 48. Metathoracic gland peritreme branching:** 0 – unbranched; 1 – branched. The branched state (either Y- or T-shaped) is present in the Vianaidinae (Schuh et al. 2006, fig. 5; Guidoti et al. 2020, fig. 16) distinguishing these from all other miroids in which the peritreme is unbranched when present.

**Character 49. Metathoracic gland ostiole position:** 0 – between coxae exposed; 1 – laterad to coxae. In the Tinginae (e.g. Cassis et al. 2019, fig. 51F) and Cantacaderinae (e.g. Schuh et al. 2006, fig. 6B), the ostiole is found laterad of the coxae, in comparison to the Xylastodorinae where this is found in close association with the metacoxae, as in *Latebracoris norfolcensis* (e.g. Fig. 8h).

**Character 50. Metathoracic gland evaporative area presence:** 0 – present; 1 – absent. Within the Miroidea the presence of evaporative areas is typical in most Miridae and Vianaidinae, with a few evaporative bodies in some Cantacaderinae (Schuh et al. 2006, fig. 6B). Evaporative bodies are absent in the Xylastodorinae, as in *Latebracoris norfolcensis* (Fig. 8h).

**Character 51. Dorsolateral abdominal tergites:** 0 – present; 1 – absent. Schuh and Štys (1991) first codified the fusion or separation of the abdominal dorsolateral tergites and mediotergites. This character has been used in all subsequent phylogenetic analyses (Lis 1999; Schuh et al. 2006, 2009; Weirauch et al. 2019) and herein.

**Character 52. Abdominal spiracle I:** 0 – present; 1 – absent. This character was first codified in Schuh and Štys (1991) and modified by Schuh et al. (2009). On the basis of

the latter authors, abdominal spiracle 1 in Thaumastocoridae is codified as absent herein, in contrast to presence in the other miroid taxa in this analysis.

**Character 53. Abdominal male SVIII: 0 – symmetrical; 1 – asymmetrical.** In reference to the asymmetry of the male genitalia in Thaumastocoridae, abdominal SVIII has not been recognised to also be asymmetrical, as in *Latebracoris norfolcensis* (Fig. 8b, 11a). This is not so in other Miroidea, including the fossil taxon *Thaumastotisingis areolatus*, where this is apparently symmetrical based on the images in Heiss and Golub (2015, fig. 1–3).

**Character 54. Male abdominal SVIII posterolateral region: 0 – not expanded caudally; 1 – lobiform.** Lis (1999, fig. 9, 24) illustrated a lobiform abdominal SVIII posterolaterally in Cantacaderinae. We interpret abdominal SVIII of *Thaumastotisingis areolatus* in the images in Heiss and Popov (2002) to be homologous.

**Character 55. Pygophore shape: 0 – conical to suboval; 1 – tubiform.** The pygophore of the Thaumastocoridae is diagnostic and unique within the Heteroptera, where it is tubiform and mostly apically asymmetrical (Fig. 11a–c). The conical shape of the pygophore is homologous in Tingidae and Miridae, although typically with exaggerated asymmetry in the latter.

**Character 56. Pygophore position: 0 – broad; 1 – lateral, narrow; 2 – medial, narrow.** The tubiform pygophore in Thaumastocoridae is articulated to either side of abdominal SVIII, as in *Latebracoris norfolcensis* (Fig. 8b, d). In *Thaumastotisingis areolatus* the articulation appears medial but not as broad as in other Tingidae or is confounded as in some Cantacaderinae where the posterolateral angles of abdominal SVIII are strongly projected caudally (see Character 54).

**Character 57. Paramere symmetry and presence: 0 – symmetrical; 1 – asymmetrical; 2 – left paramere only; 3 – obsolete.** In the Tingidae the parameres are symmetrical with fine scale differences in shape. Asymmetry in the parameres is pronounced in the Miridae (Cassis and Schuh 2012; Schuh and Weirauch 2020). In the Thaumastocorinae, the parameres are either absent (Xylastodorinae; e.g. Fig. 11b) or only the left is present (Thaumastocorinae; e.g. Noack et al. 2011, fig. 18).

**Character 58. Parameres midline position: 0 – not overlapping on midline; 1 – overlapping on midline.** In the Tingidae the parameres are symmetrically overlapping on the midline (e.g. Cassis et al. 2019, fig. 51B), whereas in the Miridae the parameres are either not medially contiguous or

asymmetrically overlapping. This character is coded inapplicable for the Thaumastocoridae given the presence of a left paramere at most (e.g. Noack et al. 2011, fig. 18).

**Character 59. Proctiger shape: 0 – cap-like, unarmed; 1 – cap-like, armed, single spine; 2 – subquadrate.** The proctiger in the Tingidae (e.g. Cassis et al. 2019, fig. 48G) is subhemispherical and symmetrical and like that found in the Miridae. In the Thaumastocoridae the proctiger is oval and cap-like and with a spine in *Latebracoris norfolcensis* (Fig. 11b, c).

**Character 60. Female external genitalia presence: 0 – present (lacinate); 1 – absent.** The absence of external female genitalia in the Thaumastocoridae (e.g. Fig. 12b) contrasts with the lacinate-type external genitalia found in the Miridae and Tingidae (e.g. Cassis et al. 2019, fig. 51H).

**Character 61. Ventrolateral plates IX: 0 – contiguous/subcontiguous on midline; 1 – short, widely separated.** The large and contiguous lateroventral IX plates are characteristic of the Miridae (Davis 1955) and the Tingidae (Drake and Davis 1960; Cassis et al. 2019, fig. 51H). The plates are short and narrowly ventralised in Xylastodorinae, as in *Latebracoris norfolcensis* (Fig. 9d).

**Character 62. Subgenital plate presence: 0 – present; 1 – absent.** The subgenital plate is present in Miridae and Tingidae (see citations in Character 61), and absent in Thaumastocoridae (Fig. 12b).

**Character 63. Medioposterior region of female abdominal SVII: 0 – not projected; 1 – projected medially.** In Thaumastocoridae the abdominal SVII is large and projected mediocaudally over the female genitalia (Fig. 12b).

**Character 64. Lateral oviduct reservoirs: 0 – absent; 1 – present.** Van Doesburg et al. (2010, fig. 40) reported on the presence of ball-like reservoirs near the base of each of the lateral oviducts in *Proxylastodoris kuscheli* that have also been found in *Latebracoris norfolcensis* (Fig. 12c). Lis (1999, fig. 31) reported similar structures in the lateral oviducts in *Allocader cordatus*, albeit lacking a common oviduct.

## Phylogenetic analyses

### Recent taxa partition analysis

The equal weights phylogenetic analysis resulted in a single minimal tree, with a tree length of 103, consistency index of 0.8543 and retention index of 0.9616. The implied weights (IW) analysis resulted in a single minimal tree with the same topology for K3, 5, 7 and 10 and differs minorly from the EW tree (i.e. variable position of *Xylastodoris luteolus*). The EW and IW trees have the same fit values.

The IW K3 tree for the Recent taxa partition is given in Fig. 13. In total, 19 of the 23 nodes in the IW tree have >50% resampling support. The major suprageneric findings in the Recent taxa partition analysis are as follows:

(1) The Miridae are sister to the Thaumastocoridae + Tingidae with 100% symmetric resampling support; (2) the Thaumastocoridae + Tingidae sister-group relationship is supported by a 64% resampling value and eight uncontradicted synapomorphies, including orthodox (e.g. 17-1, apex of mandibular stylets with rounded transverse elevations; 32-1, two segmented tarsi; 37-1, absence of a dorsal arolium; 45-0, hemelytral membrane without veins or cells) and new (28-1, globose coxae; 36-1, apex of second tarsomere with linguiform process; 38-1, median flexion line elongated) synapomorphies; (3) Thaumastocorinae + Xylastodorinae sister-group relationship is supported by a 99% resampling value, and 12 uncontradicted and one contradicted synapomorphies, including orthodox (3-1, dorsalisated mandibular plates; 51-1, fused dorsolateral and medial abdominal tergites; 52-1, absence of abdominal spiracle 1; 55-1, pygophore tubiform; 56-1, lateralised articulation of pygophore; 60-1, absence of female external genitalia) and new (1-3, hemelytra with short setiferous punctures; 53-1, asymmetry of male abdominal SVIII; 59-0, cap-shaped proctiger; 61-1, ventrolateral plates IX reduced; 63-1, medioposterior region of female abdominal SVII projected) synapomorphies; (4) Xylastodorinae monophyly is supported by a 93% resampling value, and three uncontradicted synapomorphies (22-2/3, projected anterolateral angles of pronotum; 42-1, costal area explanate and not areolate; 57-3, absence of parameres); (5) Thaumastocorinae monophyly is supported by a 98% resampling value and five uncontradicted synapomorphies, including orthodox (18-1, first labial segment short and dilated; 31-1, presence of a tibial appendix; 47-0, metathoracic gland efferent system absent) and new (9-1, rounded preocular region; 33-1, reduced tarsi) synapomorphies; and (6) Tingidae monophyly is supported with 93% resampling support, and two uncontradicted (26-1, prosternum laminate; 38-2, median flexion line obsolete) and three contradicted (25-1, prosternum sulcate; 27-1, pterothoracic sternal margins laminate; 34-1, parempodia short and setiform) synapomorphies, with the subfamilial relationships of (Vianaidinae (Tinginae (Phatnomatinae + Cantacaderinae))). The tingid subclade less the Vianaidinae has 100% resampling support, with ten uncontradicted and one contradicted synapomorphies. Each of the three tingid subfamilies Tinginae, Cantacaderinae and Phatnomatinae have >65% resampling and synapomorphy support.

Four of the ingroup relationships of the Xylastodorinae are with >50% resampling support, but lacking in uncontradicted synapomorphy support aside from the two Eastern Hemisphere taxa *Latebracoris norfolcensis* and *Thaicoris sedlaceki*. The sister-group relationship of the latter two species is supported by three uncontradicted synapomorphies of the head (7-1, separation of mandibular plates from clypeus; 8-3, antenniferous tubercles large; 10-1, spindle-shaped clypeus).

The Thaumastocorinae ingroup relationships are uncertain, with the two *Thaumastocoris* species nested within *Baclozygum*, and *B. depressum* sister to *T. hackeri* + *T. petilus*, bringing into question the monophyly of *Baclozygum*.

### Recent plus fossil taxa partition analysis

The EW analysis resulted in a single minimal tree, with length of 109, and consistency index of 0.8073 and retention index of 0.9503. This data partition was re-run with the IW routine applied in TNT, to assess the fit of the tree, resulting in a single minimal tree with the same topology for  $K = 3, 5, 7$  and  $10$ , with length of 110, and consistency index of 0.8090 and retention index of 0.9503. The IW topology was subject to symmetric resampling based on 10 000 replications, with >50% support for all the family-group sister relationships. The IW K3 tree for the Recent plus fossil taxa partition is shown in Fig. 14.

There was no impact of the inclusion of the four fossil taxon on family-group monophyly of Recent taxa (cf. Fig. 13 and 14). The position of the four fossil taxa is as follows: (1) *Thaumastotising areolatus* is nested within the Tingidae, and as sister to (Tinginae + Phatnomatinae) Cantacaderinae, supported by a resampling value of 53% and three uncontradicted synapomorphies: 42-2, costal area aerolate; 43-1, presence of a subcostal area; 46-1, areolate hemelytra; (2) *Proxylastodoris gerdae* is nested in the Xylastodorinae with 91% resampling support, with three of the same character state supports in the Recent taxa partition analysis (above) (22-2/3, 35-1 and 42-1). It is, however, sister to the remaining representatives of the subfamily and not to *P. kuscheli* but without character or resampling support and (3) *Discocoris dominicanus* and *Paleodoris lattini* are nested in the clade with the two Recent *Discocoris* species, with 60% resampling support, and one uncontradicted (22-1, greatly projected and rounded anterolateral angles of pronotum) and one contradicted (4-1, mandibular plates flat to concave) synapomorphies.

### Palm specialism

The palm associations for eight Xylastodorinae species are given in Fig. 15 and Table 2, confirming palm specialism at a transoceanic scale (van Doesburg et al. 2010). All but one of the palm bugs with documented palms are host plant specific, with *Discocoris drakei* reported from two genera and five palm species, in the subfamilies Arecoideae and Ceroxyloideae. *Discocoris* is the most species-rich xylastodorinae genus (5 spp.), not restricted to any one neotropical lineage of palms and occurs on five different tribal-level palms lineages, belonging to subfamilies Arecoideae, Calamoideae and Ceroxyloideae. All six palm genera on which *Discocoris* occur are restricted to the Neotropical region but belong to distantly related palm lineages. *Discocoris fernandezii* is found on a palm species from the subfamily Calamoideae and tribe Lepidocaryeae that is distantly related from the Arecoideae that harbour the remaining

**Table 2.** Xylastodorinae species palm host association, palm subfamily and tribe, biogeographic regions of palm tribe and country of origin for xylastodorine-palm species interaction.

Xylastodorinae species	Palm species	Areceaceae subfamily: tribe	Palm tribe distribution	Insect-plant distribution
<i>Discocoris drakei</i>	<i>Oenocarpus bacaba</i> Mart.	Arecoideae: Euterpeae	Neotropical	Brazil
	<i>Oenocarpus bataua</i> Mart. <sup>A</sup>	Arecoideae: Euterpeae	Neotropical	Peru
	<i>Oenocarpus distichus</i> Mart.	Arecoideae: Euterpeae	Neotropical	Brazil
	<i>Oenocarpus mapora</i> H.Karst.	Arecoideae: Euterpeae	Neotropical	Brazil
	<i>Phytelephas</i> Ruiz & Pav. sp.	Ceroxyloideae: Phytelaphae	Neotropical	Peru
<i>Discocoris fernandezi</i>	<i>Mauritia flexuosa</i> L.f.	Calamoideae: Lepidocaryeae	Neotropical, Afrotropical	Brazil
<i>Discocoris imperialis</i>	<i>Socratea montana</i> R.Bernal & A.J.Hend.	Arecoideae: Iriateae	Neotropical	Colombia
<i>Discocoris kormilevi</i>	<i>Butia yatay</i> (Mart.) Becc.	Arecoideae: Cocoseae	Neotropical, Afrotropical	Venezuela
<i>Discocoris vianai</i>	<i>Euterpe edulis</i> Mart.	Arecoideae: Euterpeae	Neotropical	Argentina
<i>Latebracoris norfolcensis</i>	<i>Rhopalostylis baueri</i> (Hook.f.) H.Wendl & Drude)	Arecoideae: Areceae	Southwest Pacific	Norfolk Island
<i>Proxylastodoris kuscheli</i>	<i>Burretiokentia vieillardii</i> (Brongn. & Gris) Pic.Serm	Arecoideae: Areceae	Southwest Pacific	New Caledonia
<i>Xylastodoris luteolus</i>	<i>Roystonea regia</i> (Kunth) O.F. Cook	Arecoideae: Roystoneaeae	Neotropical	Cuba, Florida

Host association records for *Discocoris drakei* and *D. fernandezi* are from Couturier *et al.* (1998, 2002); *D. drakei* – *Phytelephas* sp. from Schuh (1975); *D. imperialis* from Slater and Schuh (1990); *D. vianai* from Kormilev (1955); *Latebracoris norfolcensis*, in this work; *Proxylastodoris kuscheli* from van Doesburg *et al.* (2010); *Xylastodoris luteolus* from Barber (1920).

<sup>A</sup>Species interaction first recorded as *Jessenia bataua*.

xylastodorines. Most Xylastodorinae species, including the Neotropical and Southwest Pacific species are associated with the subfamily Arecoideae that is the most diverse for the palm family Areceaceae, with 14 tribes and 61 genera. The Neotropical species *Xylastodoris luteolus* occurs on only one palm species, *Roystonea regia* that is native to Cuba and widely planted as an ornamental in southern Florida.

Both the Southwest Pacific xylastodorine species (*Proxylastodoris gerdae* and *Latebracoris norfolcensis*) occur on palms of the highly speciose tribe Areceae that is widespread in the Eastern Hemisphere from Africa–Madagascar through Asia to the Indo-Pacific and Australia but does not occur in the Neotropics. *Proxylastodoris gerdae* occurs on *Burretiokentia*, a genus restricted to New Caledonia that belongs to the subtribe Basselininae that is restricted to Lord Howe, New Caledonia, Vanuatu, Fiji and Solomons. *Latebracoris* occurs on *Rhopalostylis* that belongs to the subtribe Rhopalostylidinae comprising two genera ranging from Lord Howe and Norfolk islands to New Zealand, and the Kermadec and Chatham Island archipelagos.

In Fig. 15, the host palms and xylastodorine-affiliated species (aside from *D. fernandezi*) are mapped to an abridged version of the modern suprageneric phylogeny of the Areceaceae by Baker and Dransfield (2016). This demonstrates that the Xylastodorinae on current knowledge, aside

from *D. fernandezi*, exhibit host plant conservatism at the subfamilial level, for both Neotropical and southwest Pacific xylastodorines. At the tribal level, the associations are restricted to 4 of the 14 Arecoideae tribes and this does not support an hypothesis of preferential host switching, with a caveat of the likelihood of sampling inadequacy.

For a subset of the palm–palm bug associations (Table 2), the sister-group palm tribes Euterpeae and Areceae each harbour a pair of Neotropical and Southwest Pacific xylastodorines respectively (see Fig. 15). This establishes that the palm hosts of the Southwest Pacific xylastodorines are not shared with Neotropical relatives at the tribal level.

## Discussion

### Biology

#### Natural history

*Latebracoris norfolcensis* is similar to *Discocoris* spp. and *Proxylastodoris kuscheli* within the Xylastodorinae in that adults and nymphs are found on reproductive structures of palms rather than on leaves, as in *Xylastodoris luteolus* (Weissling *et al.* 2012). *Latebracoris norfolcensis* and *Discocoris drakei* (Couturier *et al.* 2002) have the most

detailed biological information within the subfamily, both of which exhibit ecomorphological and lifestyle similarities, including: (1) cryptozoic and dorsoventrally flattened body; (2) cling tightly to plant surface; (3) found in palm cupule depressions (cf. Fig. 3d and 4 with Couturier *et al.* 2002); and (4) eggs oviposited in the fissure between the cupule rim and the base of the flower or fruit that rests in the cupule.

These two species exhibit differences in life cycle strategy that correspond with palm reproductive phenology. A palm inflorescence is a large structure and development through flowering, fruiting, fruit fall and final shedding can occur over many months. *Discocoris drakei* are early flower feeders. In this species, adults fly to young inflorescences when flowers first open, where eggs are laid and hatchlings feed only on flowers. Hatchlings vacate the palm host by flight a month later as adults before fruit has developed (Couturier *et al.* 2002). We could not study the activity of *Latebracoris norfolcensis* at early flowering stage because no palms were in flower during fieldwork. However, insecticide spraying of infructescences with young (white), medium (green) or old (red) fruit consistently yielded catches of adults of both sexes and all nymphal instars. This indicates that *L. norfolcensis* has continuous, overlapping life stages and possibly generations that persist for the lifespan of an inflorescence or infructescence. This hypothesis is supported by the fact that the dark greyish-brown adults of *L. norfolcensis* are camouflaged against the brown perianth scales of the palm host (Fig. 3a–c) that are a feature of mature fruit. In contrast, the much paler *Discocoris drakei* adults resemble the white flowers and rachillae of early inflorescences of the palm host. This is also supported by the location of eggs of *L. norfolcensis* that are inserted into the fissure around the base of mature fruit, inferring that nymphs do not feed on flowers. *Discocoris drakei* inserts eggs into the minute fissure in soft tissues around the base of small unopened flowers, whereas the fissure used by *L. norfolcensis* is wider and bounded by the tough, mature tissues of the rachilla and petiole scale. This may explain why *L. norfolcensis* glues eggs in position with a copious deposit of adhesive secretion that may be an adaptation for life on mature infructescences. Egg adhesive was not noted for *Discocoris* species and in the wider Thaumastocoridae this has only been recorded as a superficial device to anchor eggs to leaf surfaces in a few thaumastocorine species (Kumar 1964; Hill 1988).

In good seasons, mature palms may flower each time a leaf is shed resulting in an individual palm having several inflorescences of different ages, with the youngest at the top of the series. This was conspicuous in the *Rhopalostylis baueri* palms on Norfolk Island at the time of our fieldwork with some having four infructescences at different developmental stages (e.g. Fig. 2d and see caption). This indicates that the population of *L. norfolcensis* on a palm may not disperse often to infest new palms but can simply move upwards on the same individual palm and infest progressively younger fruiting structures. Our observation of adults

clustering on the outside of a soon-to-open spathe further up the palm from an older inflorescence may be an example of this behaviour (Fig. 2c). *Discocoris drakei* are frequent fliers since life on an individual palm is brief. We did not observe *L. norfolcensis* in flight, but wing buzzing and capture in a malaise trap, and no evidence of wing shortening indicate that these are capable of dispersion. Continuous sessile populations on one palm over long periods may not often need flight.

*Discocoris drakei* feed on flowers whereas the precise feeding site of *L. norfolcensis* is not clear. When living on fruit-bearing rachillae there are only two options: the rachilla surface or the fruit surface. Adults usually rest on the hard dried petiolar scales and one was seen to apparently be feeding on the rachilla surface from the pose in Fig. 3b. Nymphs were almost invisible but occasionally seen on the rachilla surface. First instars hatching from the eggs would emerge directly onto the rachilla surface, therefore the rachilla surface is the most likely feeding site. Presumably the palm vascular system would be transmitting a rich flow of nutrients to the fruit, at least during the fruit growth period and this supports the rachilla feeding site hypothesis.

### Palm specialism and sampling inadequacy

In this work we verify the hypothesis of palm specialism for Recent Xylastodorinae (Couturier *et al.* 1998, 2002; Cassis *et al.* 1999) with the inclusion of palm host records for the Southwest Pacific species *Proxylastodoris kuscheli* (van Doesburg *et al.* 2010) and *Latebracoris norfolcensis*. In Fig. 15 we show in *Discocoris*, the only multi-species xylastodorinae genus, that these are not restricted to any one Neotropical lineage of palms. The best-known species of *Discocoris*, *D. drakei*, is known from four species of the palm genus *Oenocarpus* but also an unrelated palm species in the genus *Phytelephas* from Peru (Schuh 1975) (Table 2). Couturier *et al.* (2002) postulated that *D. drakei* is an *Oenocarpus* specialist but this may be influenced by the association with multiple cultivated foodcrop species of this palm genus. This may have unnaturally expanded the host range of *D. drakei* and encounters of the species by insect collectors. All the other xylastodorines are host plant-specific (Table 2) but more survey is needed to verify that these are not oligophagous or polyphagous, and to test whether restricted host breadth is an artefact of sampling inadequacy.

The strongly supported sister-species relationship of *Latebracoris norfolcensis* and *Thaicoris sedlaceki* (Fig. 13 and 14) predicts that the host of the latter is a palm species. This is a South-East Asian xylastodorine from two widely separated localities: (1) '50 km N of Trak' Thailand (Kormilev 1969) and (2) 'Ciantar 1000 m, 20 km N of Bandung' Java (Heiss and Popov 2002). If this is a palm feeder then the elongated body may indicate that the species is a leaf-feeder like the elongated *Xylastodoris luteolus*, rather than an inflorescence feeder, as in the oval species of *Discocoris*, *Latebracoris* and *Proxylastodoris*. In our

phylogenetic analysis, *Xylastodoris luteolus* is sister to *Latebracoris norfolcensis* + *Thaicoris sedlaceki* but this is not supportive of a leaf feeding prediction, given that the relationship is without symmetric resampling support. By contrast, the fossil species *Paleodoris lattini* is elongated, yet is nested within the oval body shape of *Discocoris* with resampling support (Fig. 13 and 14) but its position is compromised by a lack of genital characters that could be codified.

Numerous xylastodorine species are known from few specimens, indicating that collection has been serendipitous, as was the initial collection of *Latebracoris norfolcensis*. Considering the crypsis of xylastodorines on inflorescences and infructescences, high out of reach of orthodox collecting techniques, the probability of discovery of new xylastodorine species on more palm species is high, particularly with the application of the novel xylastodorine collecting methods designed for palm bugs in this work (Fig. 2). This is particularly the case in the Southwest Pacific where xylastodorine discovery has occurred in only the past 10+ years and the presence of xylastodorines in South-East Asia is restricted to only two specimens of *Thaicoris sedlaceki*, both without host plant data. We predict that other palms of the Areceae may serve as hosts for the latter species, given the tribe's diversification in the Indomalayan bioregion and the tribal group upon which the related *L. norfolcensis* and *P. kuscheli* feed.

## Biogeography and conservation

### Biogeographic connections

The discovery of two Xylastodorinae endemic species in the Southwest Pacific brings into question the origins and diversification of the subfamily. Van Doesburg *et al.* (2010) discussed this for *Proxylastodoris kuscheli* based on temporally disconnected and alternative hypotheses about the origins of the New Caledonia biota in general; viz. the dispersalist Pliocene derivation and post-Palaeocene submergence v. the Gondwanan vicariance hypotheses (see Edgecombe and Giribet 2009 for discussion). Van Doesburg *et al.* (2010) came to no conclusion about the two models but suggested that present-day xylastodorine distribution may be a result of extinction and the Southwest Pacific occurrence may be a case of relictualism. These authors, by recognising *P. kuscheli* as a living fossil (because the congener *P. gerdæ* is a Baltic amber fossil), also suggested that Xylastodorinae may have been widespread in the Eastern Hemisphere during the Cenozoic. The discovery of *Latebracoris norfolcensis* herein not only fulfills that prediction but also specifically adds Norfolk Island to the xylastodorine puzzle, an oceanic island that is both remote and comparatively recent in age, ~3 million years old (Jones and McDougall 1973). Furthermore, our recognition that *Latebracoris norfolcensis* and *Thaicoris sedlaceki* are sister-species supports the notion that Recent

xylastodorines are currently more widespread (van Doesburg *et al.* 2010; Schuh and Weirauch 2020) but likely undiscovered in the Eastern Hemisphere, with the latter species being present west of Wallace's line.

The biogeographic connections of the xylastodorines between the Indo-Australian and Neotropical bioregions is an open question without the benefit of phylogenomics and divergence dating. The absence of xylastodorine-palm associations offers another avenue of enquiry. Van Doesburg *et al.* (2010) highlighted the stasis of xylastodorine-palm affiliation at a suprageneric level on the opposite sides of the Pacific and speculated that long distance dispersal for both lineages was unlikely. The mapping of all xylastodorine-palm records (Fig. 15) to the palm tribal phylogeny of Baker and Dransfield (2016) reveals no overlap of palm associations at the tribal level. This does however show that the *Discocorisdrakei*—*Oenocarpus* palm species and Southwest Pacific xylastodorine associations are shared between the sister palm tribes Euterpeae and Areceae respectively (Fig. 15). Dowe (2010) reported on the first fossil palm pollen records in Australia and New Zealand from the Palaeocene (c. 60 Ma), and that palms were diverse in the Eocene—Palaeocene but with decline in palm diversity and distribution with the onset of aridity in the late Miocene. Palm genera, including *Rhopalostylis* were also suggested to possibly have been present as an autochthonous element on the Australian continent prior to the Miocene. Pole (1994) argued that the Norfolk Island flora is a result of dispersal, with connections to New Zealand and that the flora shares the palm species *Rhopalostylis baueri* with the Kermadec Islands, the host of *Latebracoris norfolcensis*.

### Conservation of *Latebracoris norfolcensis*

The narrow range endemism of *Latebracoris norfolcensis* within the 460-ha area of Norfolk Island National Park, coupled with the possible impacts of cleared vegetation and invasive species (Director of National Parks 2010, 2018), requires consideration under the IUCN Red List methodology (International Union for Conservation of Nature 2023). The vulnerability of the species may satisfy the area and extent of occupancy criteria. This would likely be assessed as data deficient, requiring future sampling in forest remnants outside the Norfolk Island National Park and more extensive sampling within the reserve.

## Morphology and systematics

### Nymphal and egg morphological similarities in the Xylastodorinae

The Western Hemisphere taxa (*Xylastodoris luteolus* and *Discocoris* spp.) within Xylastodorinae notably have nymphs with two abdominal scent glands and eggs without a circle of erect micropylar processes around the perimeter of the operculum. In comparison, the two Southwest Pacific species, *Proxylastodoris kuscheli* and *Latebracoris norfolcensis*

have nymphs with only one scent gland and eggs with a prominent circle of erect micropylar processes. Although characters of both egg and nymphs have differences between east and west taxa, observations of more taxa are required prior to their inclusion in phylogenetic analyses.

### Challenges in homologising genital and forewing characters in the Miroidea

In both our analyses, without (Fig. 13) and with (Fig. 14) fossil taxa, the Tingidae + Thaumastocoridae relationship is supported, with corroborated resampling and synapomorphy support. None of the eight synapomorphies are of the genitalia or venation of the forewing. Given the importance of these character systems in heteropteran systematics in general, we discuss below difficulties in the homologisation, with the prospect that future resolution will verify the sister-group relationships in the Miroidea presented herein.

The asymmetrical abdominal SVIII and pygophore in Thaumastocoridae are unlike any in the Heteroptera, let alone the Miroidea. Likewise for females, with the absence of external female genitalia, enlarged abdominal SVII and absence of a subgenital plate, indicating specialised mating and oviposition behaviour, and undoubtedly in relation to the laminophile habits. Female thaumastocorids lack an ovipositor for the species investigated and the bursa copulatrix is sac-like without sclerotisation. In comparison, the external genitalia of the Miridae are alike, with a flap-like subgenital plate and a lacinate ovipositor overlapped by the eighth and ninth ventrolateral tergites (Davis 1955; Drake and Slater 1957). Even more perplexing, the sperm storage organs in the three miroid families are highly divergent. In the Miridae the sperm storage organ is a large, sac-like structure attached broadly to the bursa copulatrix and is referred to as the seminal depository (Davis 1955). In the Tingidae there are competing hypotheses, with the so-called paired pseudospermathecae leading into the bursa copulatrix (Drake and Davis 1960; Lis 1999) that are alternatively interpreted as accessory glands (Livingstone and Yacoub 1990; Schuh and Weirauch 2020). In the Thaumastocoridae there are no such organs leading into the bursa copulatrix and there are ball-like structures near the base of each of the lateral oviducts instead that we refer to as reservoirs but are of unknown function.

Forewing homology across the three target families is also vexed and this is true more broadly for the Heteroptera (Schuh and Weirauch 2020) and Hemiptera (Nel *et al.* 2012). Foremost in the Miroidea is the challenge of homologising the Tingidae forewing components, with specialised areolation and carination, with those of the Miridae and Thaumastocoridae. This is confounded in the Tingidae due to competing hypotheses of forewing venation by Drake and Davis (1960) and Lis (1999). Zhang *et al.* (2005) proposed using the fossil taxon *Ignotingis mirifica* Zhang, Golub, Popov & Shcherbakov, 2005 (Ignotingidae) forewing venation,

essentially as a ground plan but we found the application to Recent taxa of little use.

Equating the most anterior vein that is posteriad to the wing margin in Miridae and Thaumastocoridae with that of Tingidae is currently at an impasse. These have been named as R + M in Miridae (cf. Schuh and Slater 1995) and subcosta in Tingidae (Lis 1999), under the hypothesis that the anterior forewing margin is the costal vein. This is confounded by the recognition of an area in the Cantacaderinae that is anterior to the costal area, referred to as the stenocostal area by tingid specialists (Drake and Davis 1960; Froeschner 1996), that is hypothesised to be of pre-costal origin (Lis 1999). In comparison, the R + M in Thaumastocoridae is equivalent to that named in the Miridae, with the first recognisable anterior vein posteriad to the costal margin, spatially demarcated by the adjacent median flexion line in both families (cf. Fig. 10a for *L. norfolcensis* and Schuh and Slater 1995, fig. 10.1 for Miridae).

Although we did not codify corial cells in our phylogenetic analysis, there is promise in homologising the cells in the corium of Thaumastocoridae and Tingidae. The corium has four closed cells (radial, medial and two basal) in *Latebracoris norfolcensis* (Fig. 10a). This cellular configuration is very similar to that found in all Xylastodorinae, including *Discocoris drakei* (Cassis, personal observation), *Proxylastodoris gerdae* (Bechly and Wittmann 2000, fig. 1) and *Xylastodoris luteolus* (Schuh and Slater 1995, fig. 52.2D). The Dominican fossil species *Paleodoris lattini* is similar in cell number but differs in cell area and configuration (Poinar and Santiago-Blay 1997, fig. 2). We could not homologise the corial cells of the Xylastodorinae either with the extra subdivisions that are common in the Cantacaderinae forewing (Lis 1999) or the subcostal area in Tingidae because of the apparent absence in the Miridae and Thaumastocoridae. What also appears to be confounding is the elongation of the corium in the Xylastodorinae and Tingidae, resulting in a prolonged subcostal area in lace bugs but no equivalent in the palm bugs. This also has ramifications in homologising the corium in Miridae and Thaumastocorinae with the discoidal area in Tingidae.

The xylastodorine corial cells are however very similar to those found in the fossil taxon *Golmonia pater* Popov, 1989 (cf. *L. norfolcensis*, Fig. 10a and Golub and Popov 2008, fig. 1), with the former having a disputed taxonomic alliance (Lis 1999, Thaumastocoridae; Nel *et al.* 2004, *incertae familiae*; Golub and Popov 2008, Tingidae). In the illustration of the forewing of this fossil species, there are discernible elongated costal and subcostal areas, suggesting annectant morphology between Xylastodorinae that lack a subcostal area and Tingidae. We note that Golub and Popov (2016) hypothesised a relationship between Thaumastocoridae and *G. pater* based on the corial cells but did not name either the costal or subcostal areas in their illustration.

In comparison, the forewing of Thaumastocorinae lacks corial subdivision (e.g. Noack *et al.* 2011). There are also differences between the two Thaumastocoridae subfamilies,

with the Xylastodorinae having the R + M fusing with CuA distally, extending the corium to near the apex of the forewing that differentiates this from the much shorter corium in the Thaumastocorinae.

### Classification and relationships of the Thaumastocoridae

The phylogenetic analysis herein verifies, for both taxon partitions, a monophyletic Thaumastocoridae in alignment with the hypotheses of Schuh and Štys (1991) and Weirauch *et al.* (2019). In both analyses the family has 99% resampling support and 13 supporting synapomorphies, including non-genitalic and genitalic characters, such as the highly autapomorphic characters of the asymmetrical pygophore and male abdominal SVIII, and the absence of external female genitalia and subgenital plate. These results support retention of the Thaumastocorinae and Xylastodorinae as sister taxa at subfamilial rank, and the raising of the latter by Viana and Carpintero (1981) to family rank is not supported, in alignment with the ranking argumentation of Schuh *et al.* (2006).

The Xylastodorinae is monophyletic in both phylogenetic analyses, with >90% resampling support and four synapomorphies, including the loss of both parameres. This verifies the concept of xylastodorines as a transoceanic lineage. This also establishes sister-group relationships between the South-East Asian species *Thaicoris sedlaceki* and the Norfolk Island species *Latebracoris norfolcensis*, based on three head synapomorphies. This corroborates the synonymy of the Thaicorinae with the Xylastodorinae, in accordance with Schuh and Weirauch (2020). The phylogenetic analysis of the partition with fossil taxa corroborated the monophyly of the Xylastodorinae based on the Recent taxa partition, although this was compromised by the lack of genitalic characters for fossils. Uncertainty exists in the systematic position of the genus *Proxylastodoris* that is not monophyletic in the fossil taxa partition analysis (although without genital data for the fossil *P. gerdae*) and in the Recent taxa partition analysis, with *P. kuscheli* sister to the remaining Xylastodorinae species exemplars. Neither result is supported by resampling support or uncontradicted synapomorphies. Likewise, in both analyses, the clade *Xylastodoris luteolus* (*Thaicoris sedlaceki* + *Latebracoris norfolcensis*) has no resampling support nor synapomorphies.

The Thaumastocorinae was also found to be monophyletic based on 98% resampling support and five synapomorphies, with the reduced tarsi and presence of a tibial appendix correlated, suggesting a diminution of attachment and locomotory function of the tarsi. In this work, we provide the first analysis of ingroup relationships based on two species of the three Australian genera (*Baclozygum*, *Onymocoris* and *Thaumastocoris*) but with monophyly only for *Onymocoris*. The genus *Baclozygum* is lacking a modern taxonomic treatment and study of the internal genitalia of any species, hampering diagnosis and determination of its

systematic position. The Indian genus *Wechina* Drake & Slater, 1957 was not analysed given its rarity and lack of pertinent morphological information, although this is undoubtedly a member of the Thaumastocorinae (Drake and Slater 1957; Schuh and Slater 1995; Schuh and Weirauch 2020).

The fossil subfamily Thaumastotinginae is not a member of Thaumastocoridae, despite the reported presence of pre-tarsal pseudopulvilli and asymmetrical male genitalic characters (Heiss and Golub 2015). Based on our examination of the images of Heiss and Golub (2015, fig. 3) and those of *T. areolatus* provided by Heiss (pers. comm.), we hypothesise that the pygophore is positioned centrally and not laterally as in Thaumastocoridae, and the left orientation of the pygophore may be a result of preservation. Also, the paired symmetrical parameres, that may be directed caudally as in Tingidae if the pygophoral genital opening is artefactual, are not present in Thaumastocoridae, with the left paramere present at most as in the Thaumastocorinae. The female genitalia of the second specimen of *Thaumastotingis areolatus* are unlike that of Recent Thaumastocoridae and may be of the Tingidae-type, with an ovipositor and overlapping laterotergites (see Heiss and Golub 2015, fig. 6). However, given the state of preservation and our observation of only images of the fossil, we refrained from codifying this as such.

Heiss and Golub (2015) recognised the annectant morphology of *T. areolatus*, including Tingidae characters (e.g. areolation and cells in the corium) that are not present in Recent or fossil Thaumastocoridae. In addition, there are characters that are not found in both Thaumastocoridae and Tingidae, such as the three-segmented tarsi. However we found character support for the transfer of Thaumastotinginae to Tingidae in our phylogenetic analysis (Fig. 14) but there was only modest resampling support for inclusion in the latter family. Also, we did not have the opportunity to observe the specimens directly. For this reason, we regard Thaumastotinginae as *incertae familiae* and not a member of Thaumastocoridae.

We note that the discovery of critical fossil Tingidae and allies over the past 35 years (see Schuh and Weirauch 2020 for documentation) has highlighted a rich ancient morphology (Golub and Popov 2016) that is not apparent in Recent Tingidae, including that found in fossil taxa such as the Ignotingidae (Zhang *et al.* 2005). As a result, tingidologists of both Recent (e.g. Lis 1999) and fossil (Golub and Popov 2016) taxa have recognised these within a superfamily Tingoidea that is not recognised by phylogeneticists (e.g. Weirauch *et al.* 2019; Schuh and Weirauch 2020). We recognise the benefits of integrating the classification of fossil and Recent Hemiptera, as in Szwedo (2016; including the recognition of the superfamily Tingoidea). However, a nexus between both is confounded by character inapplicability, either as preservation inadequacy or characters that are unique or cannot be codified with confidence.

In this work, we have sought to assess not only the position of *Latebracoris norfolcensis* within the Thaumastocoridae but

also test the phylogenetic relationships within the superfamily Miroidea. The classification of Miroidea: Miridae, Tingidae and Thaumastocoridae, with the latter comprising the Thaumastocorinae and Xylastodorinae, is supported.

## References

- Baker WJ, Dransfield J (2016) Beyond *Genera Palmarum*: progress and prospects in palm systematics. *Botanical Journal of the Linnean Society* **182**, 207–233. doi:10.1111/boj.12401
- Baranowski RM (1958) Notes on the biology of the royal palm bug, *Xylastodoris luteolus* Barber (Hemiptera, Thaumastocoridae). *Annals of the Entomological Society of America* **51**, 547–551. doi:10.1093/aesa/51.6.547
- Barber HG (1920) A new member of the family Thaumastocoridae. *Bulletin of the Brooklyn Entomological Society* **15**, 97–104.
- Bechly G, Wittmann M (2000) Two new tropical bugs (Insecta: Heteroptera: Thaumastocoridae – Xylastodorinae and Hypsipterygidae) from Baltic amber. *Stuttgarter Beiträge zur Naturkunde Serie B (Geologie und Paläontologie)* **289**, 1–11.
- Cassis G, Gross GF (1995) 'Zoological Catalogue of Australia. Vol. 27.3A. Hemiptera: Heteroptera (Coleorrhyncha to Cimicomorpha).' (CSIRO Publishing)
- Cassis G, Schuh RT (2010) Systematic methods, fossils, and relationships within Heteroptera (Insecta). *Cladistics* **26**, 262–280. doi:10.1111/j.1096-0031.2009.00283.x
- Cassis G, Schuh RT (2012) Systematics, biodiversity, biogeography, and host associations of the Miridae (Insecta: Hemiptera: Heteroptera: Cimicomorpha). *Annual Review of Entomology* **57**, 377–404. doi:10.1146/annurev-ento-121510-133533.
- Cassis G, Symonds C (2008) Systematics, biogeography and host associations of the lace bug genus *Inoma* (Hemiptera: Heteroptera: Tingidae). *Acta Entomologica Musei Nationalis Pragae* **48**, 433–484.
- Cassis G, Schuh RT, Brailovsky H (1999) A review of *Onymocoris* (Heteroptera: Thaumastocoridae), with a new species and notes on hosts and distributions of other thaumastocorid species. *Acta Societatis Zoologicae Bohemicae* **63**, 19–36.
- Cassis G, Symonds C, Branson L (2019) Systematics and species radiation of the sheoak lace bug genus *Epimixia* Kirkaldy (Insecta: Heteroptera: Tingidae) in Australia, New Caledonia and Papua New Guinea. *Invertebrate Systematics* **33**, 277–366. doi:10.1071/IS18040
- Cobben RH (1968) 'Evolutionary trends in Heteroptera. Part I. Eggs, architecture of the shell, gross embryology and eclosion.' (Centre for Agricultural Publication and Documentation: Wageningen, Netherlands)
- Cobben RH (1978) 'Evolutionary Trends in Heteroptera. Part II. Mouthpart-structures and feeding strategies.' (H. Veenman & B.V. Zonen)
- Couturier G, Kahn F, Padilha de Oliveira MS (1998) New evidences on the coevolution between bugs (Hemiptera: Thaumastocoridae: Xylastodorinae) and the New World Palms. *Annales de la Société Entomologique de France (N.S.)* **34**, 99–101. doi:10.1080/21686351.1998.12277765
- Couturier G, De Oliviera MSP, Beserra P, Pluot-Sigwalt D, Kahn F (2002) Biology of *Discocoris drakei* (Hemiptera: Thaumastocoridae) on *Oenocarpus mapora* (Palmae). *Florida Entomologist* **85**(1), 261–266. doi:10.1653/0015-4040(2002)085[0261:BODDHT]2.0.CO;2
- Davis NT (1955) Morphology of the female organs of reproduction in the Miridae (Hemiptera). *Annals of the Entomological Society of America* **48**, 132–150. doi:10.1093/aesa/48.3.132
- Director of National Parks (2010) 'Norfolk Island Region Threatened Species Recovery Plan.' (Department of the Environment, Water, Heritage and the Arts)
- Director of National Parks (2018) 'Norfolk Island National Park and Norfolk Island Botanic Garden Management Plan 2018–2028.' (Director of National Parks: Canberra, ACT, Australia)
- Dowe JL (2010) 'Australian palms: biogeography, ecology and systematics.' (CSIRO Publishing)
- Drake CJ, Davis NT (1960) The morphology, phylogeny and higher classification of the family Tingidae, including the description of a new genus and species of the subfamily Vianaidinae (Hemiptera: Heteroptera). *Entomologica Americana* **39**, 1–100.
- Drake CJ, Slater JA (1957) The phylogeny and systematics of the family Thaumastocoridae (Hemiptera: Heteroptera). *Annual Review of the Entomological Society of America* **50**, 353–370. doi:10.1093/aesa/50.4.353
- Edgecombe GD, Giribet G (2009) Phylogenetics of scutigermorph centipedes (Myriapoda: Chilopoda) with implications for species delimitation and historical biogeography of the Australian and New Caledonian faunas. *Cladistics* **25**(4), 406–427. doi:10.1111/j.1096-0031.2009.00253.x.
- Floater GJ (1996) The Brooks–Dyar Rule and morphometrics of the Processionary Caterpillar *Ochrogaster Zunifer* Herrich-Schäffer (Lepidoptera: Thaumetopoeidae). *Australian Journal of Entomology* **35**(3), 271–278. doi:10.1111/j.1440-6055.1996.tb01402.x
- Froeschner RC (1996) Lace bug genera of the world, I: introduction, subfamily Cantacaderinae (Heteroptera: Tingidae). *Smithsonian Contributions to Zoology* **574**, 1–43. doi:10.5479/si.00810282.574
- Goloboff PA, Catalano SA (2016) TNT version 1.5, including a full implementation of phylogenetic morphometrics. *Cladistics* **32**(3), 221–238. doi:10.1111/cla.12160.
- Golub VB, Popov YA (2008) A new species of Tingidae (Insecta: Hemiptera: Heteroptera) from the lower Cretaceous of Transbaikalia. *Paleontological Journal* **42**, 86–89. doi:10.1134/S0031030108010140
- Golub VB, Popov YA (2016) Historical development and problems of classification of the heteropteran insects of the superfamily Tingoidae (Hemiptera: Heteroptera, Cimicomorpha). *Meetings in Memory of N.A. Cholodkovsky* **66**, 1–93.
- Green PS, Wilson AJG (1994) Norfolk Island and Lord Howe Island. *Flora of Australia* **49**, 1–26.
- Guidoti M, Montemayor SI, Campos LA, Guilbert E (2020) Phylogenetic analysis and revision of the strangest lace bug subfamily Vianaidinae (Heteroptera: Tingidae). *Zoological Journal of the Linnean Society* **188**(4), 1172–1212. doi:10.1093/zoolinnean/zlz089
- Guilbert E (2001) Phylogeny and evolution of exaggerated traits among the Tingidae (Heteroptera, Cimicomorpha). *Zoologica Scripta* **30**, 313–324. doi:10.1046/j.1463-6409.2001.00069.x
- Guilbert E, Damgaard J, D'Haese CA (2014) Phylogeny of the lacebugs (Insecta: Heteroptera: Tingidae) using morphological and molecular data. *Systematic Entomology* **39**(3), 431–441. doi:10.1111/syen.12045
- Heiss E, Golub VB (2015) *Thaumastotingsis areolatus* nov. gen., nov. sp. a conspicuous new Thaumastocoridae from Baltic amber (Hemiptera: Heteroptera). *Linzer Biologische Beiträge* **47**, 529–537.
- Heiss E, Popov YA (2002) Reconsideration of the systematic position of Thaicorinae with notes on fossil and extant Thaumastocoridae (Hemiptera: Heteroptera). *Polskie Pismo Entomologiczne* **71**(3), 247–259.
- Hill L (1988) The identity and biology of *Baclozygum depressum* Bergroth (Hemiptera: Thaumastocoridae). *Australian Journal of Entomology* **27**, 37–42. doi:10.1111/j.1440-6055.1988.tb01140.x
- Holloway JD (1977) 'Lepidoptera of Norfolk Island. Their biogeography and ecology.' (Springer Science & Business Media)
- Holloway JD (1982) Further notes on the Lepidoptera of Norfolk Island, with particular reference to migrant species. *Journal of Natural History* **16**(3), 351–365. doi:10.1080/00222938200770291
- Holloway JD (1990) Guest editorial: Norfolk Island and biogeography for the nineties: Ideas from a dot on the map. *Journal of Biogeography* **28**, 113–115.
- Howard FW, Giblin-Davis R, Moore D, Abad R (2001) 'Insects on palms.' (CABI Publishing)
- International Union for Conservation of Nature (2023) The IUCN Red List of Threatened Species. Version 2022-2. Available at <https://www.iucnredlist.org>
- Jones JG, McDougall I (1973) Geological history of Norfolk and Philip islands, southwest Pacific Ocean. *Journal of the Geological Society of Australia* **20**(3), 239–254. doi:10.1080/14400957308527916
- Kerzhner IM (1981) 'Fauna of the USSR. Heteroptera of the family Nabidae. Vol. 13(2).' (Academy of Sciences USSR, Zoological Institute. Rhynchota. (N.S.): Leningrad, USSR) [In Russian]
- Kormilev NA (1955) Una curiosa familia de Hemipteros neuva para la fauna Argentina, Thaumastotheriidae (Kirkaldy, 1907). *Revista de la Sociedad Entomológica Argentina* **18**, 5–10.

- Kormilev NA (1969) Thaicatorinae, n. subfam. from Thailand (Hemiptera; Heteroptera; Piesmatidae). *Pacific Insects* **11**, 645–648.
- Kumar R (1964) Anatomy and relationships of Thaumastocoridae (Hemiptera: Cimicoidea). *Australian Journal of Entomology* **3**, 48–51. doi:10.1111/j.1440-6055.1964.tb00621.x
- Lis B (1999) Phylogeny and classification of Cantacaderini [=Cantacaderidae stat. nov.] (Hemiptera: Tingoidea). *Annales Zoologici* **49**(3), 157–196.
- Livingstone D, Yacoob MHS (1990) Female accessory glands and sperm reception in Tingidae (Heteroptera). *Proceedings: Animal Sciences* **99**, 431–446. doi:10.1007/BF03186406
- Macphail MK, Hope GS, Anderson A (2001) Polynesian plant introductions in the Southwest Pacific: initial pollen evidence from Norfolk Island. *Records of the Australian Museum, Supplement* **27**, 123–134. doi:10.3853/j.0812-7387.27.2001.1347
- Nel A, Waller A, de Ploëg G (2004) The oldest palm bug in the Lowermost Eocene amber of the Paris Basin (Heteroptera: Cimicomorpha: Thaumastocoridae). *Geologica Acta* **2**(1), 51–55.
- Nel A, Prokop J, Nel P, Grandcolas P, Huang DY, Roques P, Guilbert E, Dostál O, Szewo J (2012) Traits and evolution of wing venation pattern in paraneopteran insects. *Journal of Morphology* **273**(5), 480–506. doi:10.1002/jmor.11036.
- Nixon KC (2002) 'WinClada, Version 1.00.08. Program and Documentation.' (Cornell University Press)
- Noack AE, Cassis G, Rose HA (2011) Systematic revision of *Thaumastocoris* Kirkaldy (Hemiptera: Heteroptera: Thaumastocoridae). *Zootaxa* **3121**, 1–60. doi:10.11646/zootaxa.3121.1.1
- Pintaud JC, Baker WJ (2008) A revision of the palm genera (Arecaceae) of New Caledonia. *Kew Bulletin* **63**, 61–73. doi:10.1007/s12225-007-9009-3
- Poinar GO, Poinar R (1999) 'The amber forest: a reconstruction of a vanished world.' (Princeton University Press)
- Poinar GO, Santiago-Blay JA (1997) *Paleodoris lattini* gen. n., sp. n., a fossil palm bug (Hemiptera: Thaumastocoridae, Xylastodorinae) in Dominican amber, with habits discernible by comparative functional morphology. *Insect Systematics & Evolution* **28**(3), 307–310. doi:10.1163/187631297X00097
- Pole M (1994) The New Zealand flora – entirely long-distance dispersal? *Journal of Biogeography* **21**, 625–635. doi:10.2307/2846036
- Rentz DCF (1988) The orthopteroid insects of Norfolk Island, with descriptions and records of some related species from Lord Howe Island, South Pacific. *Invertebrate Systematics* **2**(8), 1013–1077. doi:10.1071/IT9881013
- Salmon JT (1986) 'The native trees of New Zealand.' (Reed Books: Auckland, New Zealand)
- Sanchez JA, Cassis G (2018) Towards solving the taxonomic impasse of the biocontrol plant bug subgenus *Dicyphus* (*Dicyphus*) (Insecta: Heteroptera: Miridae) using molecular, morphometric and morphological partitions. *Zoological Journal of the Linnean Society* **184**, 330–406. doi:10.1093/zoolinnean/zly005
- Schaefer CW (1969) Morphological and phylogenetic notes on the Thaumastocoridae (Hemiptera: Heteroptera). *Journal of the Kansas Entomological Society* **42**, 251–256.
- Schuh RT (1975) Wing Asymmetry in the Thaumastocorid *Discocoris drakei* (Hemiptera). *Revista Peruana de Entomología* **18**(1), 12–13.
- Schuh RT (1976) Pretarsal structure in the Miridae (Hemiptera) with a cladistic analysis of relationships within the family. *American Museum Novitates* **1976**(2601), 1–39.
- Schuh RT, Slater JA (1995) 'The true bugs of the world (Hemiptera: Heteroptera).' (Cornell University Press)
- Schuh RT, Štys P (1991) Phylogenetic analysis of cimicomorphan family relationships (Heteroptera). *Journal of the New York Entomological Society* **99**(3), 298–350.
- Schuh RT, Weirauch C (2020) 'True Bugs of the World (Hemiptera: Heteroptera): Classification and Natural History.' (Siri Scientific Press)
- Schuh RT, Cassis G, Guilbert E (2006) Description of the first recent macropterous species of Vianaidinae (Heteroptera: Tingidae) with comments on the phylogenetic relationships of the family within the Cimicomorpha. *Journal of the New York Entomological Society* **114**(1), 38–53. doi:10.1664/0028-7199(2006)114[38:DOTFRM]2.0.CO;2
- Schuh RT, Weirauch C, Wheeler WC (2009) Phylogenetic relationships within the Cimicomorpha (Hemiptera: Heteroptera): a total-evidence analysis. *Systematic Entomology* **34**(1), 15–48. doi:10.1111/j.1365-3113.2008.00436.x
- Slater JA (1973) A contribution to the biology and taxonomy of Australian Thaumastocoridae with the description of a new species (Hemiptera: Heteroptera). *Australian Journal of Entomology* **12**, 151–156. doi:10.1111/j.1440-6055.1973.tb01653.x
- Slater JA, Baranowski RM (2000) *Discocoris dominicanus*, a new species of palm bug from Dominican amber (Heteroptera: Thaumastocoridae). *The Florida Entomologist* **83**, 349–353. doi:10.2307/3496354
- Slater JA, Schuh RT (1990) A remarkably large new species of *Discocoris* from Colombia (Heteroptera: Thaumastocoridae). *Journal of the New York Entomological Society* **98**, 402–405.
- Szewo J (2016) The unity, diversity and conformity of bugs (Hemiptera) through time. *Earth and Environmental Science Transactions of the Royal Society of Edinburgh* **107**(2–3), 109–128. doi:10.1017/S175569101700038X
- Tian Y, Zhu W, Li M, Xie Q, Bu W (2008) Influence of data conflict and molecular phylogeny of major clades in Cimicomorphan true bugs (Insecta: Heteroptera). *Molecular Phylogenetics and Evolution* **47**(2), 581–597. doi:10.1016/j.ympev.2008.01.034.
- van Doesburg PH, Cassis G, Monteith GB (2010) Discovery of a living fossil: a new xylastodorine species from New Caledonia (Heteroptera: Thaumastocoridae) and first record of the subfamily from the eastern Hemisphere. *Zoologische Mededelingen* **84**, 93–115.
- Viana MJ, Carpintero DJ (1981) Una nueva especie de *Discocoris* Kormilev, 1955 (Hemiptera, Xylastodoridae). *Museo Argentino de Ciencias Naturales Bernardino Rivadavia e Instituto Nacional de Investigación de las Ciencias Naturales* **1**(4), 63–74.
- Weirauch C (2007) Hairy attachment structures in Reduviidae (Cimicomorpha, Heteroptera), with observations on the fossula spongiosa in some other Cimicomorpha. *Zoologischer Anzeiger - A Journal of Comparative Zoology* **246**, 155–175. doi:10.1016/j.jcz.2007.03.003
- Weirauch C, Schuh RT, Cassis G, Wheeler WC (2019) Revisiting habitat and lifestyle transitions in Heteroptera (Insecta: Hemiptera): insights from a combined morphological and molecular phylogeny. *Cladistics* **35**(1), 67–105. doi:10.1111/cla.12233.
- Weissling TJ, Howard FW, Meerow AW (2012) Royal Palm Bug, *Xylastodoris luteolus* Barber (Insecta: Hemiptera: Thaumastocoridae). Leaflet EENY-097, University of Florida, Institute of Food and Agricultural Sciences.
- Zhang J, Golub VB, Popov YA, Shcherbakov DE (2005) Ignotingidae fam. nov. (Insecta: Heteroptera: Tingoidea), the earliest lace bugs from the upper Mesozoic of eastern China. *Cretaceous Research* **26**(5), 783–792. doi:10.1016/j.cretres.2005.05.004

**Data availability.** The data that support this study are available in the article.

**Conflicts of interest.** The authors declare that they have no conflicts of interest.

**Declaration of funding.** This research did not receive any specific funding.

**Acknowledgements.** We are grateful to several people on Norfolk Island for help and advice. National Park Manager Nigel Greenup arranged collecting permits and welcomed us; resident retired entomologist, Glynn Maynard, photographed specimens during early winter; James Tweed collected specimens at extra localities and seasons on his permit, made some useful observations, prepared the distribution map and allowed us to use one of his photographs; and local resident Geoff Edwards showed us where good populations of palms were. Geoff Thompson at the Queensland Museum produced morphology photographs on the QM photo unit; Hannah Mathews prepared the line drawings; Marina Cheng assisted with the preparation of Fig. 13–15; Dr Randall T. Schuh (AMNH) and Derek Smith (AM) provided comparative material; and Dr Ernst Heiss provided images of *Thaumastotisingis areolatus*.

**Author affiliations**

<sup>A</sup>Evolution & Ecology Research Centre, School of Biological, Earth and Environmental Sciences, University of New South Wales, Sydney, NSW 2052, Australia.

<sup>B</sup>Department of Invertebrate Zoology, Queensland Museum, Brisbane, Qld 4000, Australia.

<sup>C</sup>PO Box 5473, Cairns, Qld 4870, Australia.